A STUDY OF SUPERCONDUCTING DOMAIN STRUCTURES USING OPTICAL POLARIZATION TECHNIQUES

by

LOWELL ROSEN

B. Eng. Phys. Cornell Univ.

(1962)

SUBMITTED IN PARTIAL FULFILLMENT
OF THE REQUIREMENTS FOR THE
DEGREE OF
MASTER OF SCIENCE
at the
MASSACHUSETTS INSTITUTE
OF TECHNOLOGY

August, 1965

Signature of Author . . . . . Signature redacted
Dept. of Physics, August 23, 1965

Certified by . . . . . Signature redacted
Thesis Supervisor

Accepted by . . . . . Signature redacted
Chairman, Departmental Committee
on Graduate Students

ABSTRACT

A STUDY OF SUPERCONDUCTING
DOMAIN STRUCTURES USING
OPTICAL POLARIZATION TECHNIQUES

by

LOWELL ROSEN

SUBMITTED TO THE DEPARTMENT OF PHYSICS
ON AUGUST 23, 1965 IN PARTIAL
FULFILLMENT OF THE REQUIREMENTS
FOR THE DEGREE OF MASTER OF
SCIENCE

The superconducting magnetic structures of Tantalum have been studied using the effect of optical Faraday rotation in Cerous Metaphosphate glass. Photographs of the Tantalum specimen are included which show both the intermediate and mixed states of the metal. The sequence of magnetization pictures show the magnetic structures as the magnetic field is first increased in one direction, decreased to zero and then increased in the opposite direction. Part of the sequence of photographs clearly indicate the phenomena of the flux-jumping characteristic of type II and hard superconductors.

Thesis Supervisor: M. W. P. Strandberg
Title: Professor of Physics

ACKNOWLEDGEMENTS

With a deep sense of appreciation the author gratefully acknowledges the very kind and sincere supervision that Professor M. W. P. Strandberg provided during the course of the thesis work. Without his able guidance and sense of humor it is doubtful whether the author could have hurdled the many obstacles which appeared during the experimental work.

Special thanks also go to Professor R. L. Kyhl and to the late Professor H. Mueller for their interest in the thesis and their many fine suggestions.

Special thanks go to Dr. R. Hensler of the Ceramics Research Department of Bausch and Lomb who gratiously supplied the sample of paramagnetic glass used in the experiment.

The author would also like to thank Professor R. Rose who provided aid in the preparation of the Tantalum and in the processing of the domain photographs.

The author is also specially indebted to J. Kiersted and W. Schwabe for their invaluable aid in constructing parts of the apparatus and supplying the needed techniques in low temperature instrumentation.

Many thanks also go to Dr. J. Andrews who gratiously supplied me with his superconducting magnet.

Last but not least the author gratefully acknowledges the consideration of the administrative officers of the Research Laboratory of Electronics.

TABLE OF CONTENTS

LIST OF ILLUSTRATIONS

CHAPTER I

INTRODUCTION

In this introductory chapter we present a short review of the basic techniques which have been tried with varying degrees of success, to provide an indication of the presence of magnetic domain structure in superconductors. For the most part these previous experiments have provided much information on the structure, motion, shape, etc. of the intermediate state as a function of temperature, magnetic field, impurity content, mechanical history. However, little of this same type of information has been obtained for the mixed state in type II superconductors. It has only been within the past year that photographs of the mixed state have been published.[1] The techniques to be described all have one thing in common - they all attempt to provide photographs, or motion pictures of the magnetic structure. These techniques are to be contrasted with those which, for example, use a magnetoresistive probe[2] to sample the magnetic field about a superconductor sitting in an external field. The probe technique, though useful at first, is highly limited in its ability to map the non-equilibrium magnetic structures associated with both the type I and type II superconductors. Moreover, the finite size of the probes will in general limit the attainable resolution of the technique. The techniques for which we do have an interest are the powder or Bitter methods and the optical Faraday rotation schemes. These will now be described in more detail.

The Powder or Bitter Methods

Using the powder technique the magnetic configuration on the surface of a superconductor is displayed by depositing a thin layer of magnetic powder on the metal's surface. If the magnetic powder is a ferromagnetic material such as iron or permalloy it will tend to accumulate on those surface regions of the superconductor which are normal. That is, the ferromagnetic particles, like iron filings on a magnet, are attracted to regions in which a magnetic field exists. Experiments using ferromagnetic powder have been carried out with some success by various Russian workers.[3] If on the other hand the powder is diamagnetic it is displaced from the normal regions of the superconductor, which contain flux, and accumulate in the superconducting regions. Experiments using this type of magnetic powder have been carried out by several American workers.[4]

Though the ferromagnetic powders can provide useful information, there are several serious objections to their use. Existing around the individual grains are large local fields which might disturb the distribution of superconducting domains. This would then produce a distorted domain structure, which may not at all be indicative of the actual magnetic structure. Moreover, the large forces between particles sitting in the regions of flux cause them to form chains and other patterns, also not indicative of the actual structure.

On the other hand diamagnetic powder is expelled from normal regions of the surface where flux passes. It remains in the

superconducting regions. When looking at the surface of a metal having this powder on it, its shiny surface shows up the normal regions while the areas covered with the diamagnetic powder show up relatively dark and indicate the superconducting domains. The only materials which possess a diamagnetism strong enough to make the technique useable are the superconductors themselves. When they are superconducting they are perfectly diamagnetic, having a zero permeability. A popular material which has been used with great success is niobium powder. This material has a superconduction transition temperature of $8.5^{\circ}K$ and a critical field of several thousand oersteds at $0^{\circ}K$. Thus, in the study of most soft superconductors the niobium is perfectly diamagnetic over all the possible ranges of temperature and magnetic field. The niobium powder as compared with the ferromagnetic material has a lower susceptibility and hence smaller stray fields and interparticle forces. Unlike the iron particles in the ferromagnetic powder the niobium grains move almost independently of eachother in the presence of a magnetic field. Moreover, when the niobium powder is in an equilibrium position it is in a region of zero field and therefore, not subjected to any magnetic forces. As a result the niobium powder causes negligible disturbance of the superconductor on which it is deposited.

Using either the ferromagnetic or diamagnetic powders it has been found that for high resolution the powder should be as fine as possible. This is particularily important in the studies of flux trapping and pinning, and in the study of the

small structures characteristic of the type I superconductors.

Optical Faraday Rotation Methods

The optical techniques employ the rotation of the plane of polarization of a monochromatic light beam as it passes through a paramagnetic material deposited on the surface of a superconductor. For such a material the optical rotation is almost a linear function of the magnetic flux passing through it. P. B. Alers has shown[5] that for the particular choice of the Ce+++ paramagnetic ion which exists in glass made from Cerium Metaphosphate the linear dependence of rotation on field strength is quite good up to field strengths of about 20,000 oerstaeds at a temperature of 1°K. Beyond this field strength the optical rotation tends to saturate at a value of about 4.76π radians (glass is 1mm thick) for a glass containing 100% Cerium Metaphosphate.

As the amount of rotation is proportional to the magnetization of a paramagnetic salt used, it would appear then, that if such a material were deposited on a superconductor showing some magnetic structure the material would be magnetized over areas of normal metal through which flux passes and unmagnetized over superconducting areas. As a result if polarized light traveling parallel to the applied field was allowed to pass through the paramagnetic material the magnetized regions would produce Faraday rotations while the unmagnetized ones would not. The Faraday effect is non-reciprocal so that the sense

of the optical rotation depends only upon the direction of the megnetic field and not on the direction of the light beam in the material. As a result the amount of optical rotation is doubled over that of a single traversal through the material when the light beam strikes the superconducting surface and is reflected back through the paramagnetic material for a second traversal. As the amount of rotation is different for light reflected off normal regions as compared to that reflected off the superconducting areas the differences in polarization can be changed into intensity variations by means of a polarization analyzer and the domain structures made visible. This particular approach has been done in the United States by Alers and DeSorbo.[1]

The Faraday effect methods have the distinct advantage over the powder techniques in that time-dependent effects can be easily followed. In the powder techniques the time-dependent effects are usually obscured by the sticking together of the individual particles (though this is greatly reduced when diamagnetic powders are used). Moreover, the Faraday technique allows one to measure quantitatively the flux density in the various regions of the magnetic structure visible on the surface of the superconductor. This immediately gives us an opportunity to measure the strength of flux lines which are pinned down by impurities or imperfections in the superconductor and to also measure the flux dentisy in the mixed state existing in type II superconductors.

CHAPTER II

MAGNETIC STRUCTURES OF SUPERCONDUCTORS

In this chapter both the intermediate state and mixed state of superconductors are described. They are compared for both type I and type II superconductors.

General Considerations

When a superconducting metal is cooled below its transition temperature its electrical resistivity vanishes. If a "small" magnetic field is impressed on the metal the flux lines are excluded from the body of the metal if the metal is superconducting. If, on the other hand, a sufficiently "large" magnetic field is applied the superconductivity will be destroyed. The transition from superconductivity to normal behavior in a magnetic field can occur abruptly only if the effective field throughout the metal is constant at all parts of the material. In practice an abrupt transition will only occur in long rods or wires where the rod axis is parallel to the applied field. For other geometries the effective field will reach the critical value at some places on the metal even though the applied field is somewhat lower. The effect of shape on the critical field can best be described by what is commonly called the demagnetization coefficient of the specimen, D. If one treats the superconductor in the presence of an external field as a magnetic body with an interior field and a magnetization such that

Outside Specimen : $B_{ext} = H_{ext} + H_s$ (H_s due to specimen magnetization)

Surface Specimen : $J_s = 0$ (J_s = current density)

Interior Specimen : $B_{int} = 0$, $H_{int} \neq 0$, $M_i \neq 0$.

then using the expression that $\bar{B} = \bar{H} + 4\pi\bar{M}$ we obtain that inside the superconductor

$$M_{int} = -\frac{1}{4\pi} H_i \qquad (2.1)$$

or that the superconductor has an ideal diamagnetic susceptibility of $-\frac{1}{4\pi}$. Moreover, we also have that the interior H field is related to the exterior H field through the relation

$$H_i = H_e - 4\pi D M_i \qquad (2.2)$$

where D is the demagnetization coefficient of the metal. Combining eqs. 2.1 and 2.2 yields

$$M_i = -H_e / 4\pi(1 - D)$$

and

$$H_i = H_e / (1 - D)$$

Typical values for D are 0 for an infinitely long cylinder with its axis parallel to the direction of the applied field; $D = \frac{1}{2}$ for an infinitely long cylinder with its axis at right angles to the applied field; and D = 1/3 for a sphere.

Consider, for instance the short cylinder shown in crossection in fig. 2.1. For this shape at very low fields the flux lines go around the outside of the sample (fig. 1a). As the greatest flux concentration occurs at the corners (actually the circumference of the ends), field penetration will begin there when the local field reaches the critical field for the particular material. When the field penetration starts around the circum-

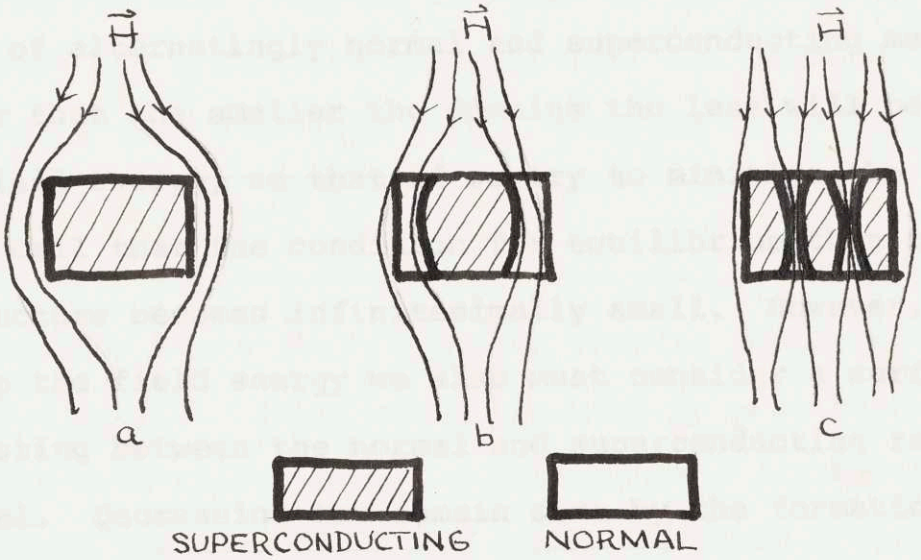

fig. 2.1 Flux distribution around a short cylinder
a. very low field
b. larger field - penetration at edges
c. intermediate state with field passing through normal regions

ference the situation is shown in fig. 2.1b. In this case the outer perimeter of the cylinder is normal while the interior still remains superconducting. Picture 2.1b, however, describes an unstable situation. It indicates that the largest fields must occur on the boundary, while farther from the center they must be smaller. For stability the local field would have just the critical value on the boundary and be somewhat larger in the normal region. To achieve the stable configuration what must happen is that the sample breaks up into a number of regions or domains of alternatingly normal and superconducting material. It is clear that the smaller the domains the less will be the magnetic field energy, so that if we try to minimize the field energy and call that the condition for equilibrium then the domain structure becomes infinitesimally small. However, in addition to the field energy we also must consider a surface energy existing between the normal and superconducting regions of the metal. Decreasing the domain size by the formation of new domains also increases the area of surface between normal and superconducting regions. This, then tends to increase the surface energy. Thus, a finite surface energy limits the smallness of the domains and in combination with the field energy determines the domain size and configuration. This mixture of normal and superconducting regions is called the intermediate state. Fig. 2.1c attempts to provide a crude picture of what the intermediate state might look like.

Magnetic Flux Structures in Superconductors

One of the basic properties of a superconductor is the reversible exclusion of flux from the metal when it becomes superconducting. That this is not a property which can be deduced from the perfect conductivity of the metal can be shown by cooling the metal, in the presence of a magnetic field, from a temperature above its transition temperature to one below it. Provided the applied magnetic field is small enough the flux lines will be excluded from the interior of the metal as it passes through the transition temperature. The London equation describing this flux exclusion effect (Meisner effect) is

$$\nabla \times \bar{J} = - (c/4\pi\lambda^2)\, \bar{H} \qquad (2.4)$$

The magnetization curve for a specimen showing the Meisner effect is shown in fig. 2.2. (This curve, as will be pointed out later, is for a so-called type I superconductor exhibiting a single critical field.) The above London equation together with the Maxwell equation $\nabla \cdot H = 0$ and the static continuity equation

$$\nabla \cdot J = 0$$

lead to

$$\nabla^2 H - \frac{1}{\lambda^2} H = 0 \qquad (2.5a)$$

and to

$$\nabla^2 J - \frac{1}{\lambda^2} J = 0 \qquad (2.5b)$$

Thus, on the surface of a superconductor H and J (field and current) decrease exponentially toward the interior with a characteristic distance, λ where

$$\lambda = \left(\frac{mc^2}{4\pi n_s e^2} \right)^{1/2}$$

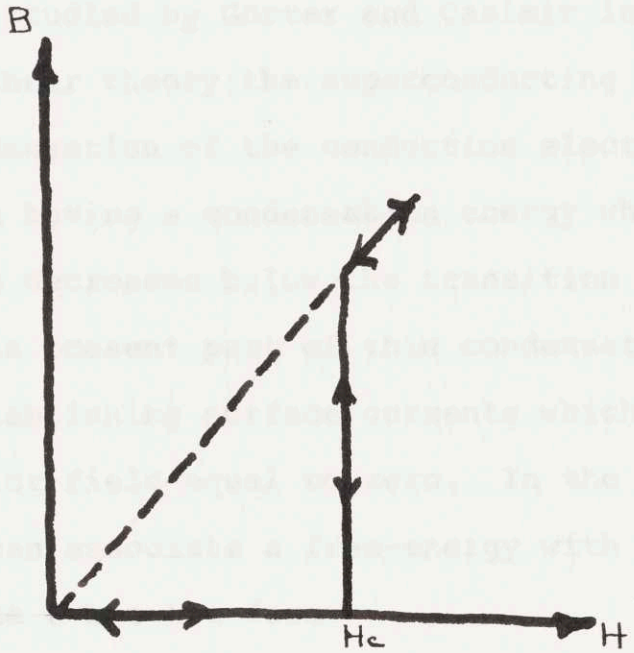

fig. 2.2 B-H characteristics of a type I superconductor

In this last equation for the characteristic distance n_s is the density of superconducting electrons. For the so-called "soft" superconductors (type I) this penetration distance is typically several hundred angstroms.

The reversibility of the Meissner effect also establishes the concept of a reversible thermodynamic transition taking place as a metal becomes superconducting. This thermodynamic approach has been studied by Gorter and Casimir in their two-fluid model. In their theory the superconducting transition is regarded as a condensation of the conduction electrons into a more ordered state having a condensation energy which increases as the temperature decreases below the transition point. When a magnetic field is present part of this condensation energy is expended in extablishing surface currents which are used to make the interior field equal to zero. In the Gorter-Casimir model we can associate a free-energy with the superconductor, G, where G has the form

$$G = -\frac{Hc^2}{8\pi} + \frac{H^2}{8\pi} \qquad (2.6)$$

(G is taken to be zero for the normal state)

Equation 2.6 thus expresses the free energy per unit volume in the presence of H. From equation 2.6 we see that since G equals zero for H equal to H_c, $\frac{Hc^2}{8\pi}$ is the magnetic-energy equivalent of the condensation energy.

For a certain class of superconductors the Meissner effect is incomplete in that magnetic flux penetrates into the

interior of the superconductor over a finite range of magnetic fields applied (even if the demagnetization factor is zero). These materials are known as "hard" superconductors or type II superconductors. Unlike the type I materials the hard superconductors often shown highly irreversible magnetizations as illustrated in fig. 2.3. However, if the hard superconductor is sufficiently strain free and pure the magnetization of the superconductor will take place reversibly over a finite range of applied fields as illustrated in fig. 2.4.

The subtle but important differences between the behavior of type I and type II superconductors can be made somewhat clearer if we introduce the Pippard coherence distance, ξ, which is essentially the spatial range over which ordering of the superconducting electrons can be altered. In the BCS theory ξ is essentially the size of the wavefunction for the superconducting electron pair. For the temperature, T, equal to 0°K it is given by ξ_o where

$$\xi_o = \frac{0.18\hbar V_f}{KT_c} \qquad (2.7)$$

(V_f is the Fermi velocity)

ξ_o is typically 10^{-4}cm for type I superconductors. Type II superconductors on the otherhand have their coherence distance limited by the normal electronic mean free path, ℓ, which may be less than 10^{-4}cm. For these materials the coherence distance ξ has the form

$$\frac{1}{\xi} = \frac{1}{\xi_o} + \frac{1}{\ell} \qquad (2.8)$$

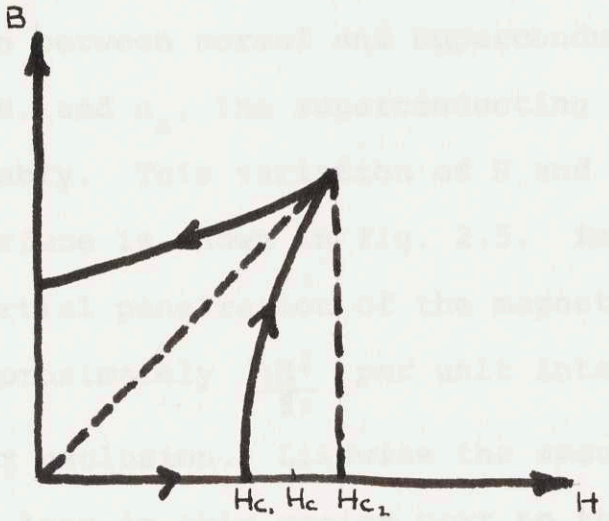

fig. 2.3 B-H characteristic of a hard superconductor exhibiting irreversible magnetization

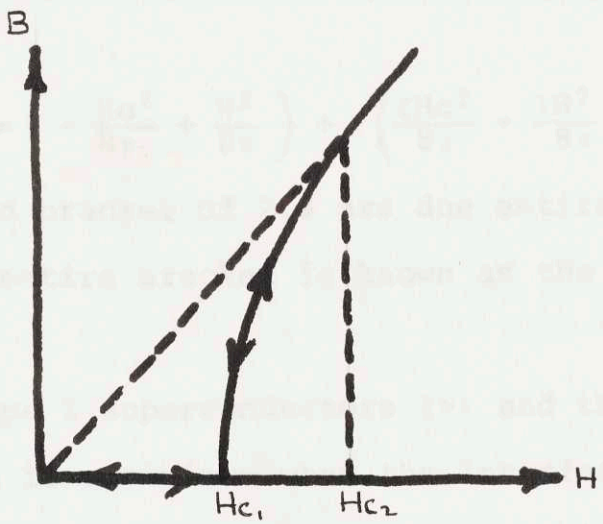

fig. 2.4 B-H characteristic of a type II superconductor exhibiting reversible magnetization

The expression for the free energy, G, that was given by eq. 2.6 correctly predicts the free energy for bulk superconductors - however, additional considerations must be looked at in the interface region between normal and superconducting areas where both the field, H, and n_s, the superconducting electron density, vary considerably. This variation of H and n_s with distance from the interface is shown in fig. 2.5. In type II superconductors the partial penetration of the magnetic field causes less energy (approximately $\frac{\lambda H^2}{8\pi}$ per unit interface area) to be expended for flux exclusion. Likewise the amount of electronic ordering is less in this region next to the interface so that the condensation energy is reduced by approximately

$$\xi Hc^2 \diagdown 8\pi$$

Thus, the free energy, G, in the interface has the following form.

$$G = \left(- \frac{Hc^2}{8\pi} + \frac{H^2}{8\pi} \right) + \left(\frac{\xi Hc^2}{8\pi} - \frac{\lambda H^2}{8\pi} \right) \quad (2.9)$$

The terms in the second bracket of 2.9 are due entirely to the interface so that the entire bracket is known as the surface energy.

For the case of type I superconductors $\xi > \lambda$ and the surface energy is positive and is a minimum when the interface area is as small as possible. This minimization can be achieved if the magnetic field is kept out of the material completely. This means that the Meissner effect represents the stable condition thermodynamically. On the other hand if $\xi < \lambda$ as is the case in

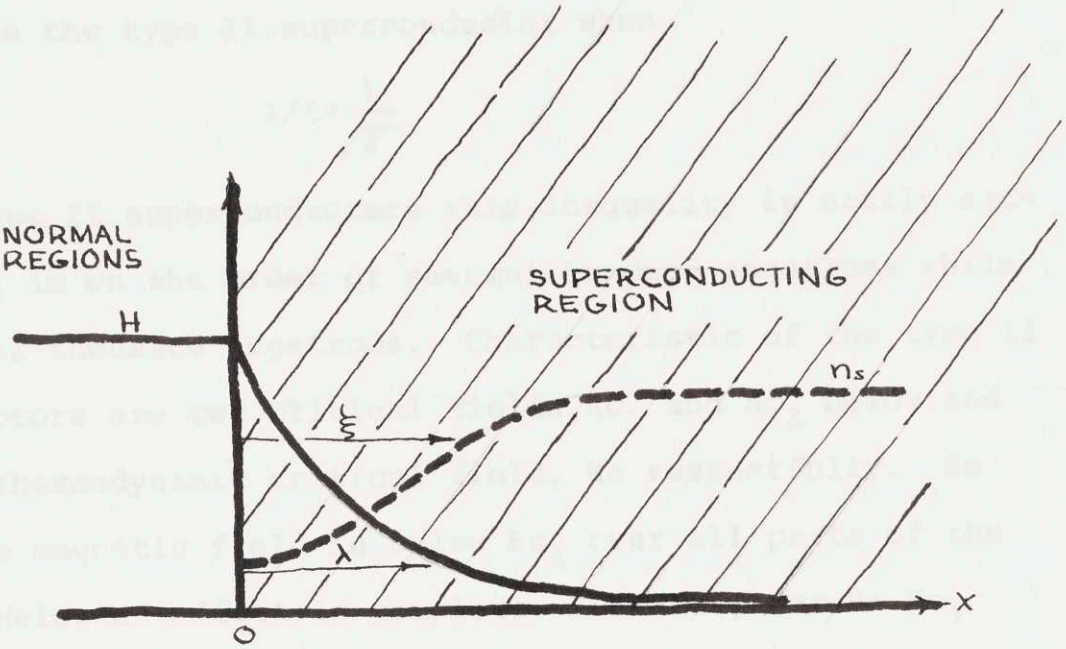

fig. 2.5 Variation of magnetic field and order parameter in the interface region λ is the London penetration depth, ξ the Pippard coherence distance

$\lambda << \xi$ for type I superconductor
$\lambda >> \xi$ for type II superconductor

type II superconductors the surface energy is negative. As a result of this, the bulk superconductor prefers to increase the interface energy by allowing the magnetic field to penetrate into the interior.

The Ginzburg-Landau theory predicts that the field will start to penetrate the type II superconductor when

$$\lambda/\xi > \frac{1}{\sqrt{2}}$$

For most type II superconductors this inequality is easily satisfied as ξ is on the order of several hundred angstroms while λ is several thousand angstroms. Characteristic of the type II superconductors are two critical fields Hc_1 and Hc_2 below and above the thermodynamic critical field, Hc respectfully. So long as the magnetic field is below Hc_1 over all parts of the metal the Meissner effect is complete. However, for $H > Hc_1$ the surface energy becomes negative and flux starts to penetrate the interior of the metal.

In the region between Hc_1 and Hc_2, called the mixed state, magnetic flux reversibly enters the type II superconductors without destroying the superconductivity. Observed values of Hc_2 have been as high as 200,000 oe while the largest observed Hc is less than 2,000 oe. Two different descriptions of the electromagnetic structure of the mixed state have been formulated. The first is an array of flux filaments with cores of nearly normal material, while the second is an array of flux lamellae. In the absence of imperfections, impurities, etc., it is generally believed that a pure type II material should form a

pure type II material should form a mixed state containing flux filaments in some order. What these filaments are like can probably be ascertained by assuming that

$$\lambda/\xi >> 1$$

and using the London equation for H modified by a singularity at the filament center. That is,

$$\nabla^2 H - \frac{1}{\lambda^2} H = \phi_o \, \delta(\bar{r}) \qquad (2.10)$$

ϕ_o represents a quantum of flux equal to

$$\frac{hc}{2e} = 2\times10^{-7} \text{ Gauss - cm}^2$$

Solutions[7] of equation 2.10 are indicated graphically in fig. 2.6.

As indicated above the average flux in a specimen is $B = n\phi_o$. As H increases B does likewise and eventually the flux lines start to overlap when $B > \phi_o/4\lambda^2$. When the distance between flux lines becomes equal to 2ξ the specimen is completely normal. The field at which the superconductivity disappears is Hc_2 where

$$Hc_2 = \sqrt{2}\,(\lambda/\xi)Hc \sim \frac{\phi_o}{4\xi^2}$$

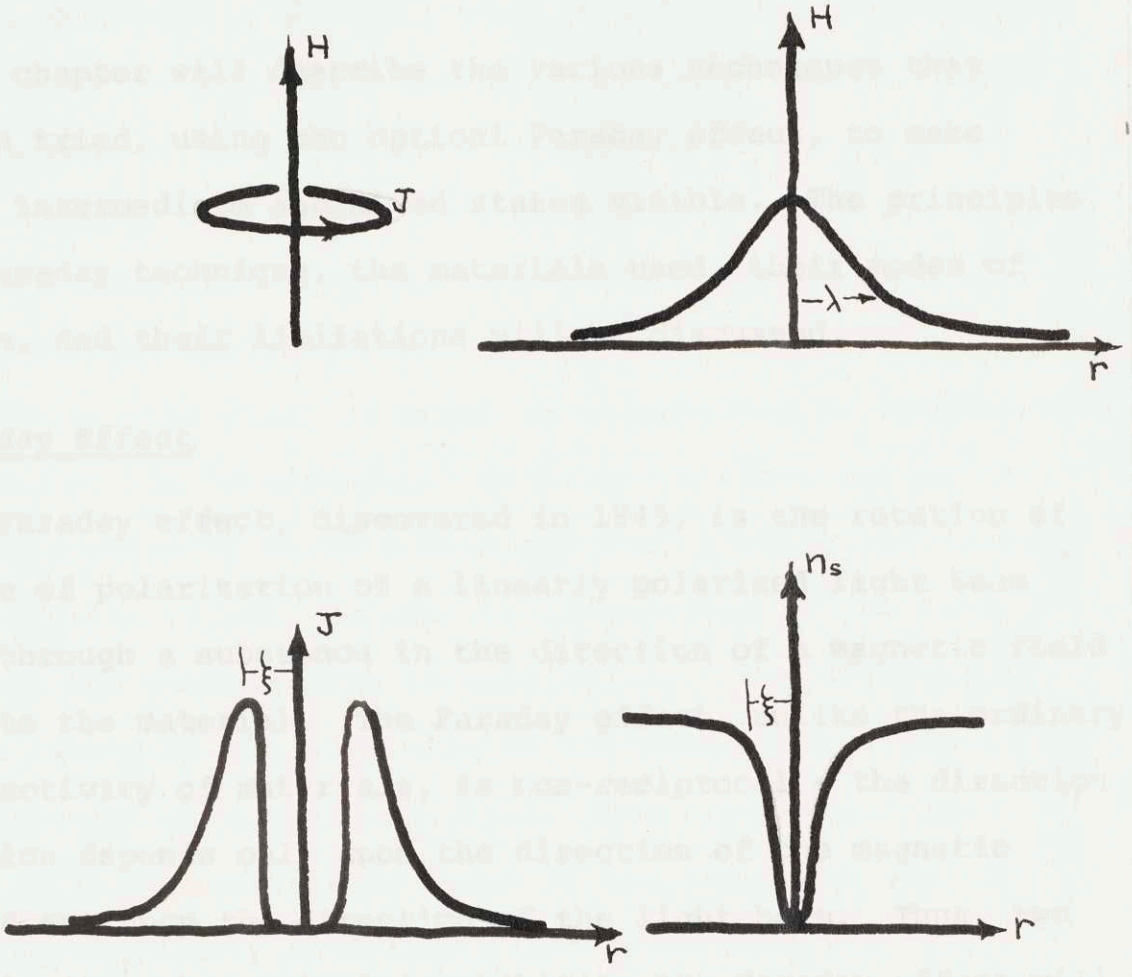

fig. 2.6 Structure of a flux line in the mixed state - core of filament is of normal material and is of size $\sim \xi$, it also contains most of the flux. Flux extends into superconducting region by a distance $\sim(\lambda - \xi)$.

CHAPTER III

OPTICAL TECHNIQUES

This chapter will describe the various techniques that have been tried, using the optical Faraday effect, to make both the intermediate and mixed states visible. The principles of the Faraday technique, the materials used, their modes of operation, and their limitations will be discussed.

The Faraday Effect

The Faraday effect, discovered in 1845, is the rotation of the plane of polarization of a linearly polarized light beam passing through a substance in the direction of a magnetic field applied to the material. The Faraday effect, unlike the ordinary optical activity of materials, is non-reciprocal - the direction of rotation depends only upon the direction of the magnetic field and not upon the direction of the light beam. Thus, two traversals through a material exhibiting the Faraday effect will produce a net rotation of $2\theta_o$ and not zero (where θ_o is amount of rotation per single traversal). For materials such as water or glass at room termperature the rotation is best described by the relation

$$\theta_o = V \cdot H \cdot L \qquad (3.1)$$

H is the magnetic field
L is the length of the Faraday material
V is a material constant giving the rotation/length/field (called the Verdet constant)

The situation for a glass rod in the field of a solenoid wrapped about it is shown in fig. 3.1. Typically, at room temperature, the Verdet constant is so small that even for fields of several thousand gauss the rotations for glass or water having lengths of a centimeter or so is measured in minutes of arc.

After Faraday's discovery it became evident that the optical rotation was connected with the magnetization of the material used. In 1928 it was shown that the rotation could be attributed to two effects, the first of which is independent of temperature and was called the "diamagnetic" rotation (a misonomer as the effect has nothing to do with diamagnetism) - while the second, the paramagnetic effect, depends on temperature in the same way as does the paramagnetic susceptibility. The diamagnetic effect is caused by the splitting of the absorption lines of the Faraday material in a magnetic field, thus producing a difference, Δn in the refractive index of the substance for two oppositely, circularly polarized light beams (see fig. 3.2). This Δn is now related to the rotation by the relation

$$\theta_o = \frac{L}{\lambda_o} \Delta n \ \pi \qquad (3.2)$$

L is the length of the Faraday material
λ_o is the wavelength in vacuum of light used
Δn is the refractive index difference

This diamagnetic effect (shown by all transparent substances) has a positive sign, meaning the rotation is in the same direction as the current in the coils producing the magnetic field (see fig. 3.1).

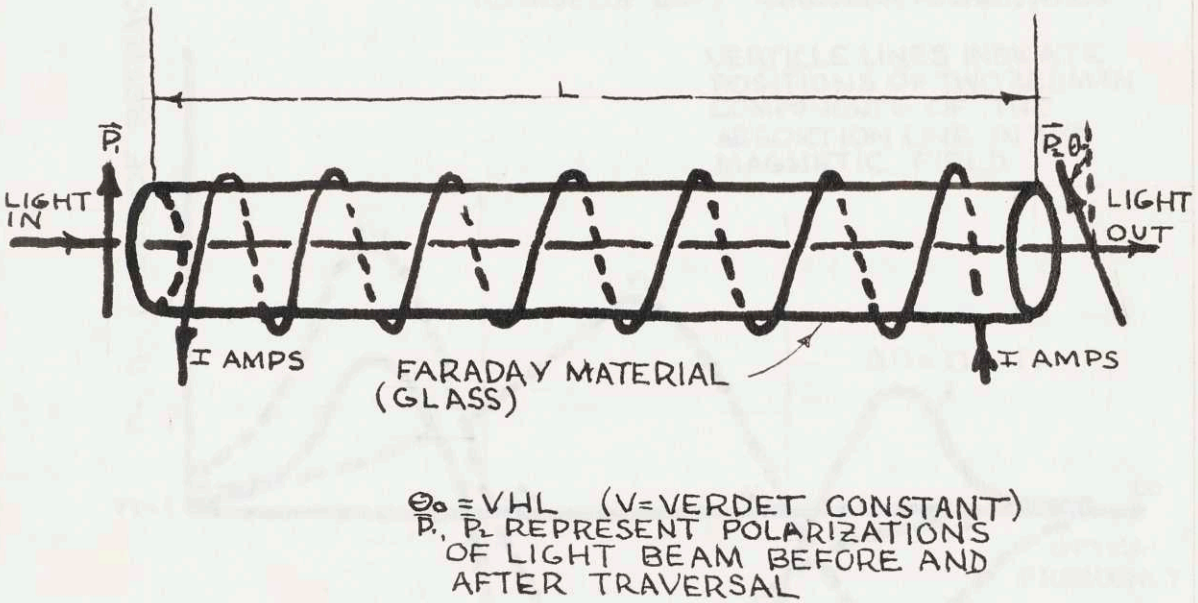

fig. 3.1 Description of Faraday effect in a glass rod.

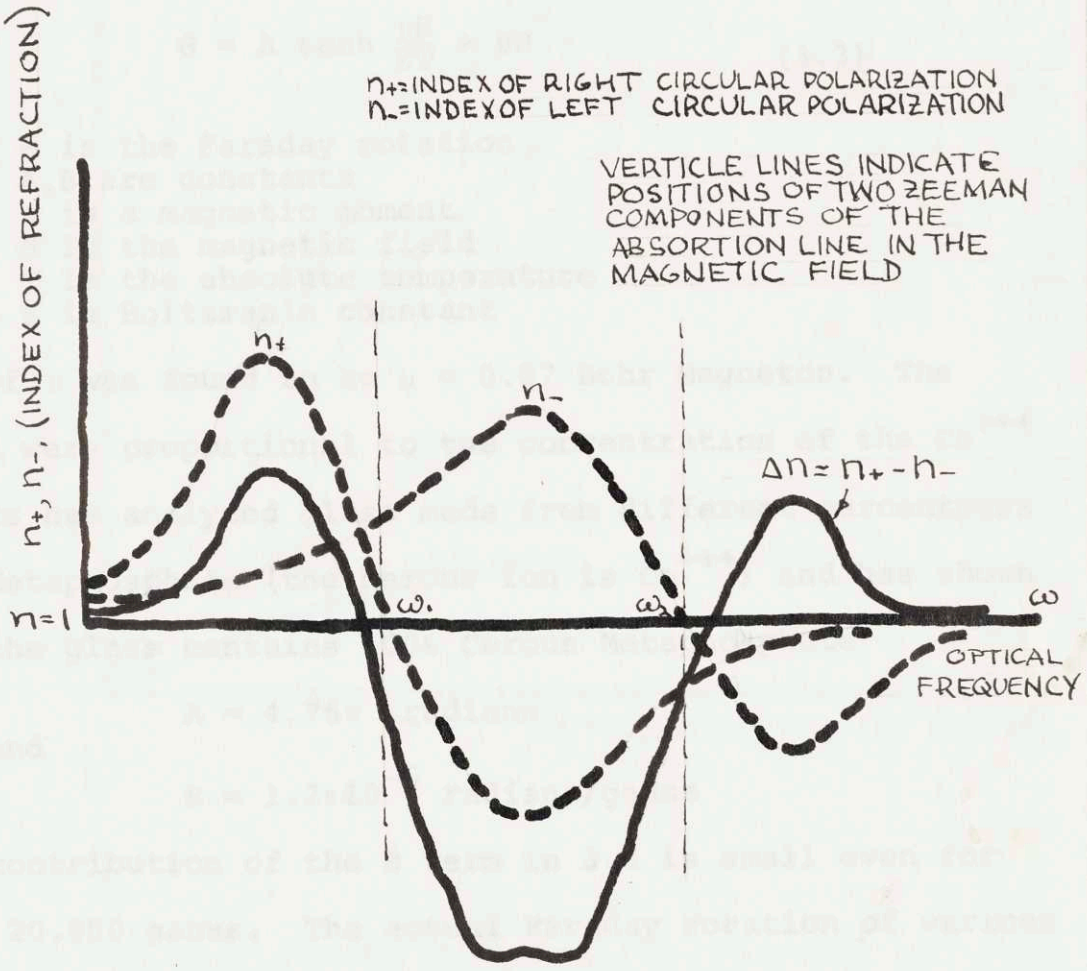

fig. 3.2 Difference in indices for two circular polarizations in a Faraday material subjected to a magnetic field.

At low temperatures the populations of the various electron levels change causing the paramagnetic effect. According to Becquerel, de Haas, and van der Handel, the Faraday rotation of Ce^{+++} (a rare earth paramagnetic ion) can be fitted to an equation of the form

$$\Theta = A \tanh \frac{\mu H}{KT} + BH \qquad (3.3)$$

Θ is the Faraday rotation
A,B are constants
μ is a magnetic moment
H is the magnetic field
T is the absolute temperature
K is Boltzman's constant

The value of μ was found to be $\mu = 0.87$ Bohr Magneton. The values of A were proportional to the concentration of the Ce^{+++} ion. Allers has analyzed glass made from different percentages of Cerous Metaphosphate (the cerous ion is Ce^{+++}) and has shown that when the glass contains 100% Cerous Metaphosphate

$$A = 4.76\pi \text{ radians}$$

and

$$B = 1.2\pi \times 10^{-6} \text{ radians/gauss}$$

Thus, the contribution of the B term in 3.3 is small even for H equal to 20,000 gauss. The actual Faraday rotation of various Cerous Metaphosphate glasses (due to Alers) is shown in Fig. 3.3. The salts of Cerium containing the cerous or Ce^{+++} ion are particularily useful in Faraday rotation studies - unlike most of the paramagnetic salts of the other rare earth elements the Cerium salts show very little color, thus, reducing the amount of light absorption.

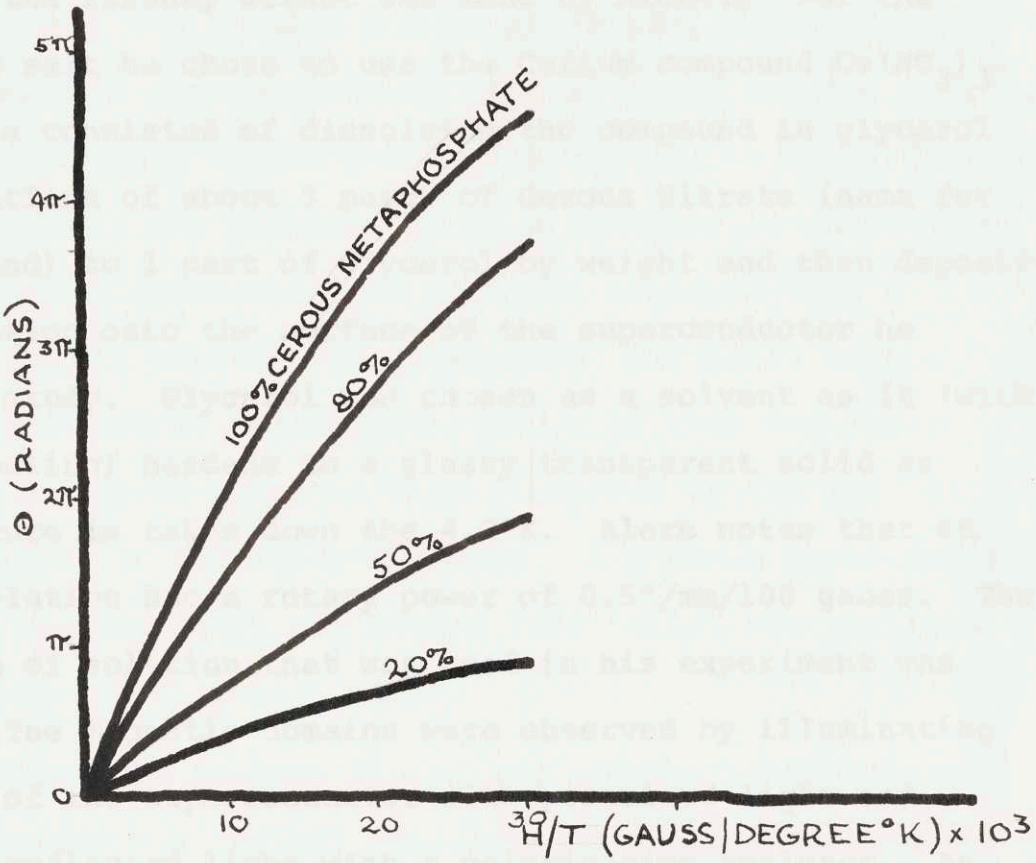

fig. 3.3 Faraday rotation Θ vs ratio of magnetic field to absolute temperature for various cerous metaphosphate glasses.

The Liquid Technique in Observing Superconducting Domains

The first attempt to view the superconducting intermediate state using the Faraday effect was made by Alers.[8] For the paramagnetic salt he chose to use the Cerium compound $Ce(NO_3)_3$. His technique consisted of dissolving the compound in glycerol in concentrations of about 3 parts of Cerous Nitrate (name for above compound) to 1 part of glycerol by weight and then depositing the solution onto the surface of the superconductor he intended to study. Glycerol was chosen as a solvent as it (with very slow cooling) hardens to a glassy transparent solid as the temperature is taken down the 4.2°K. Alers notes that at 1.8°K the solution has a rotary power of 0.5°/mm/100 gauss. The actual depth of solution that was used in his experiment was about 3mm. The magnetic domains were observed by illuminating the surface of the superconductor with polarized light and viewing the reflected light with a polarization analyzer. As the paramagnetic glycerol solution was relatively thick the normal areas showed up as white ring-like regions while the superconducting areas showed up as black - neither the black or white areas showed any finer details other than the gross ring patterns.

The Paramagnetic Glass Technique

The second attempt to view the intermediate and mixed states of a superconductor was undertaken by DeSorbo.[1] His

technique involved the use of a thin piece (0.2mm thick) of Cerium Metaphosphate glass showing a rotary power of 1.5-2.5°/mm/100 gauss at 1.4°K. The glass has several advantages over the solution - first, the glass has a higher rotary power and can therefore, be made correspondingly thinner (this has the decided advantage of yielding higher resolution as will be pointed out shortly), secondly the glycerol shows a tendency to crack into small pieces thus distorting the pictures (witness Aler's photographs in his article[7]), and thirdly, the glass offers a uniform thickness of paramagnetic material over the superconductor as compared with the uneven surface of the liquid solution sitting on the superconductor. A noneven paramagnetic layer leads to stationary but random (spacially) fluctuations in θ_o and hence polarization noise.

The optics used in both Aler's and DeSorbo's experiments are quite similar - a typical schematic of their arrangements is shown in fig. 3.4.

Fringing Magnetic Fields and Image Resolution

In both Aler's and DeSorbo's experiments the attainable image resolution was limited by the size of the paramagnetic layer over the superconductor rather than by the external photographic optics. The entire Faraday rotation scheme depends upon the assumption that the magnetic field distribution within the paramagnetic layer is approximately equal to the field distribution inside the magnetic domains of the superconductor.

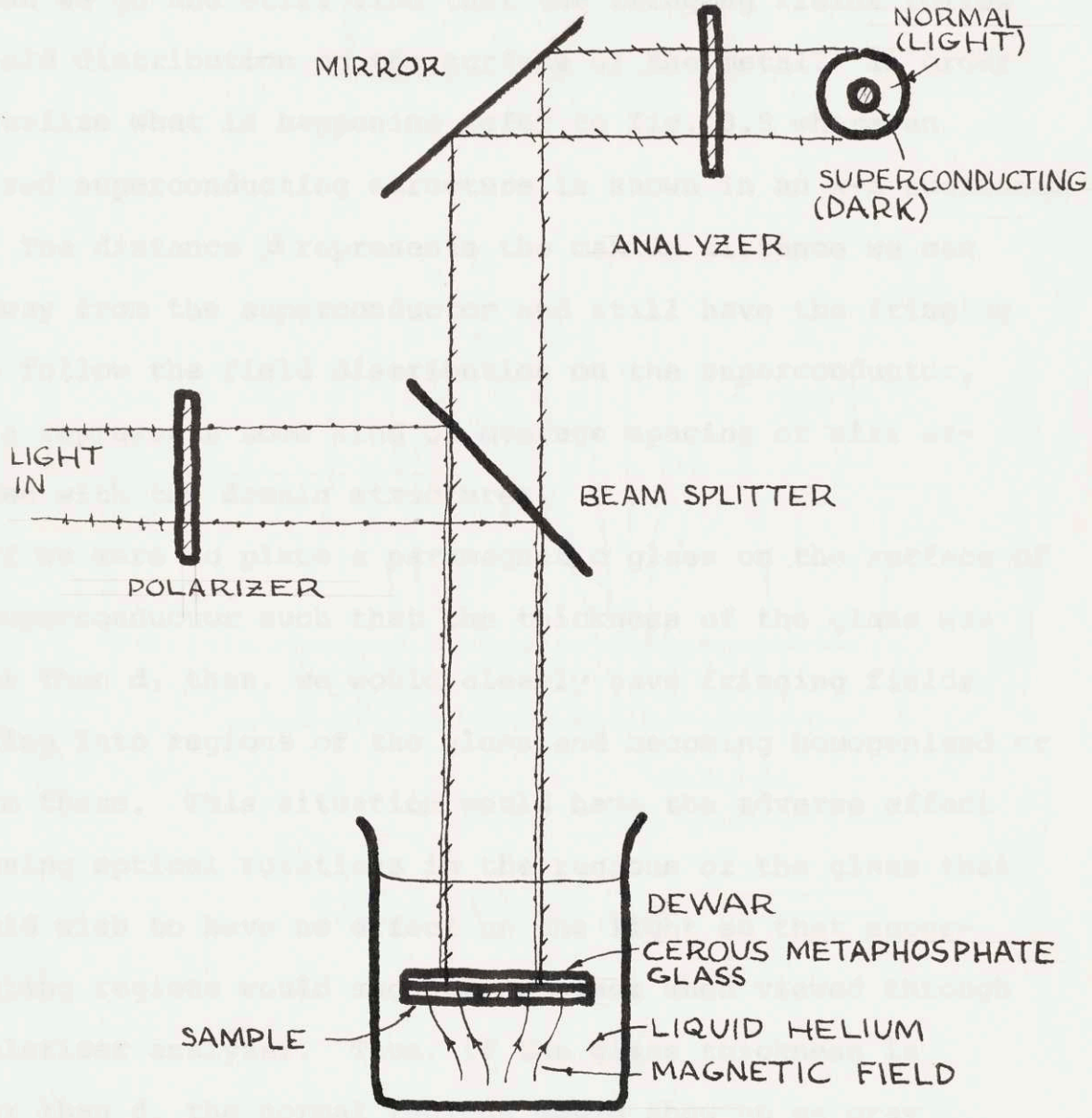

fig. 3.4 Optical arrangement for observing superconducting domains.

Thus, an important question is, if we are given a certain distribution of magnetic field on the surface of the superconductor (due to alternatingly normal and superconducting domains as in the intermediate state) how far above the surface can we go and still find that the fringing fields follow the field distribution on the surface of the metal? In order to visualize what is happening refer to fig. 3.5 where an idealized superconducting structure is shown in an x-z sectional view. The distance d represents the maxium distance we can move away from the superconductor and still have the fringing fields follow the field distribution on the superconductor, while a represents some kind of average spacing or size associated with the domain structures.

If we were to place a paramagnetic glass on the surface of this superconductor such that the thickness of the glass was greater than d, then, we would clearly have fringing fields extending into regions of the glass and becoming homogenized or uniform there. This situation would have the adverse effect of causing optical rotations in the regions of the glass that we would wish to have no effect on the light so that superconducting regions would show up as black when viewed through the polarizer analyzer. Thus, if the glass thickness is greater than d, the normal regions would show up as gray rather than black when viewed through the analyzer. Image contrast between normal and superconducting regions would go down making them more difficult to see and likewise, image resolution would go down.

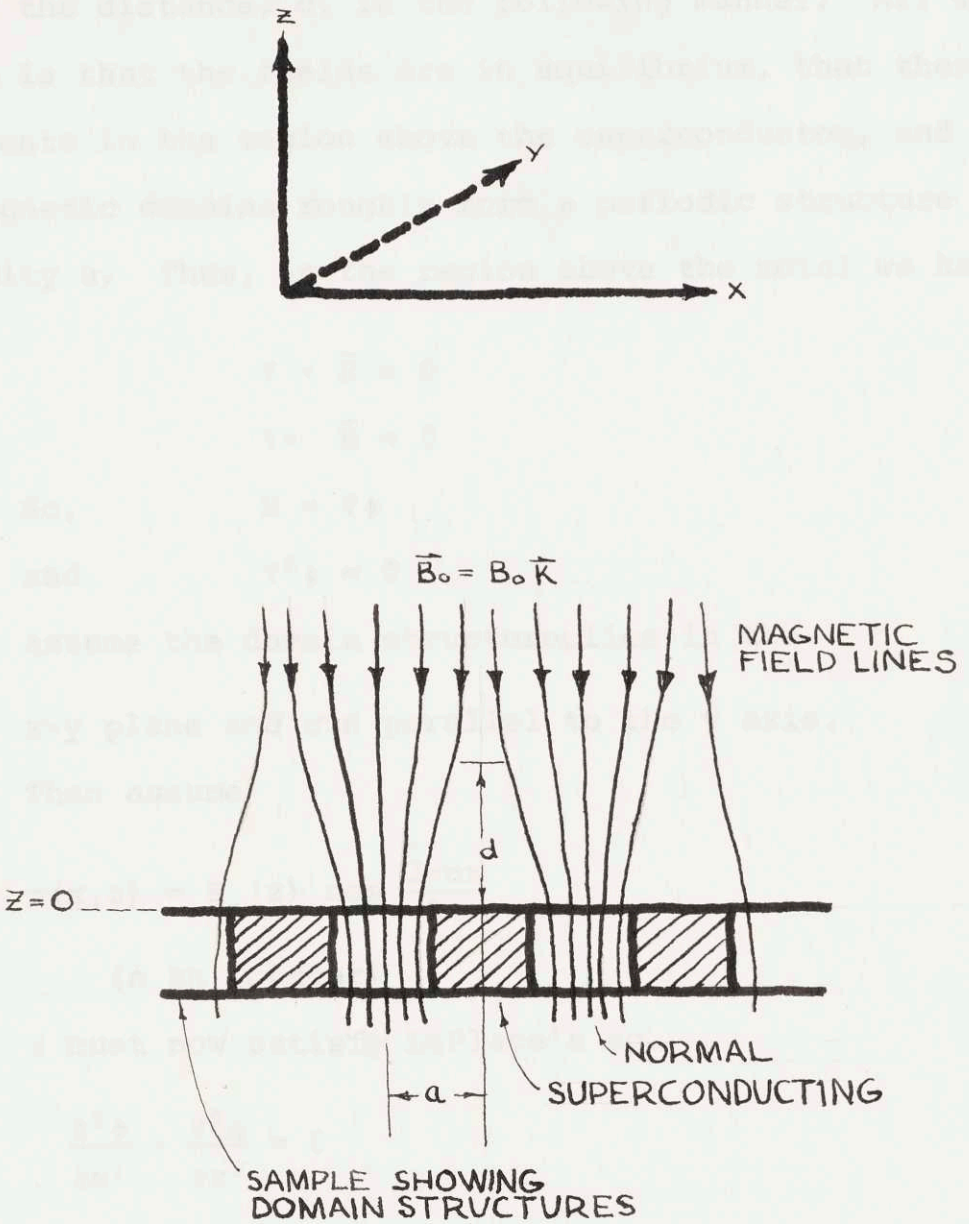

fig. 3.5 Fringing field lines about an ideal intermediate state structure.

If we know what the spacing, a, is then we can obtain an estimate of the distance, d, in the following manner. All we need assume is that the fields are in equilibrium, that there are no currents in the region above the superconductor, and that the magnetic domains roughly form a periodic structure of periodicity a. Thus, in the region above the metal we have

$$\nabla \cdot \bar{B} = 0$$

$$\nabla \times \bar{B} = 0$$

So, $B = \nabla\phi$

and $\nabla^2\phi = 0$

assume the domain structures lies in the x-y plane and run parallel to the y axis.

Then assume

$$\phi(x,z) = F_n(z) \cos \frac{2\pi n x}{a}$$

(n an integer)

ϕ must now satisfy LaPlace's eq.

$$\frac{\partial^2\phi}{\partial x^2} + \frac{\partial^2\phi}{\partial z^2} = 0$$

plugging in assumed form of ϕ.

get

$$\frac{-4\pi n^2}{a^2} F_n(z) \cos\frac{2\pi n x}{a} + \frac{d^2 Fn}{dz^2} \cos\frac{2\pi n x}{a} = 0$$

$\therefore$ $F_n(z)$ satisfies eq.

$$\frac{d^2 F_n}{dz^2} = \frac{4\pi^2 n^2}{a^2} F_n$$

$$\therefore F_n(z) = A_n e^{-\frac{2\pi n}{a} z}$$

Thus, for n = 1 (first harmonic) field falls by $e^{-2\pi}$ so that d must be <a, if glass is to give good resolution. (There is of course still a uniform field component

$$\phi_o = B_o z)$$

CHAPTER IV

EXPERIMENTAL SETUP AND HARDWARE

This chapter will consider the various components that made up the experimental setup for observing the magnetic domain structures. Schematics will be given for the special circuits used as well as photographs of the actual equiptment.

Optical Setup

The arrangement and type of optical equipment used in the experiment is quite similar to that employed by DeSorbo and Aler. A simplified optical schematic is shown in fig. 4.1. Not shown on the schematic are the details of the dewar head used to provide the hermetic windows for viewing and allowing light to enter the dewars.

The polarizers come from General Scientific and are marked so that rotations can be measured down to about 1/2°. The interference filter is a commercial item from Baird Atomic of Cambridge. It is a multilayer dielectric filter having a transmission peak at the Mercury green line, 0.546u, a peak transmission of 40% and a line width of about 60Å. The beam splitter is nothing more than a rectangular piece of glass. The camera used to record the images of the superconducting surface was a 35mm single lens reflex fitted with a 180mm telephoto lens. The lens was fitted with a 1/2 inch extension tube to allow focusing down to about 4 feet. The film used was Tri-X rated ASA-1200

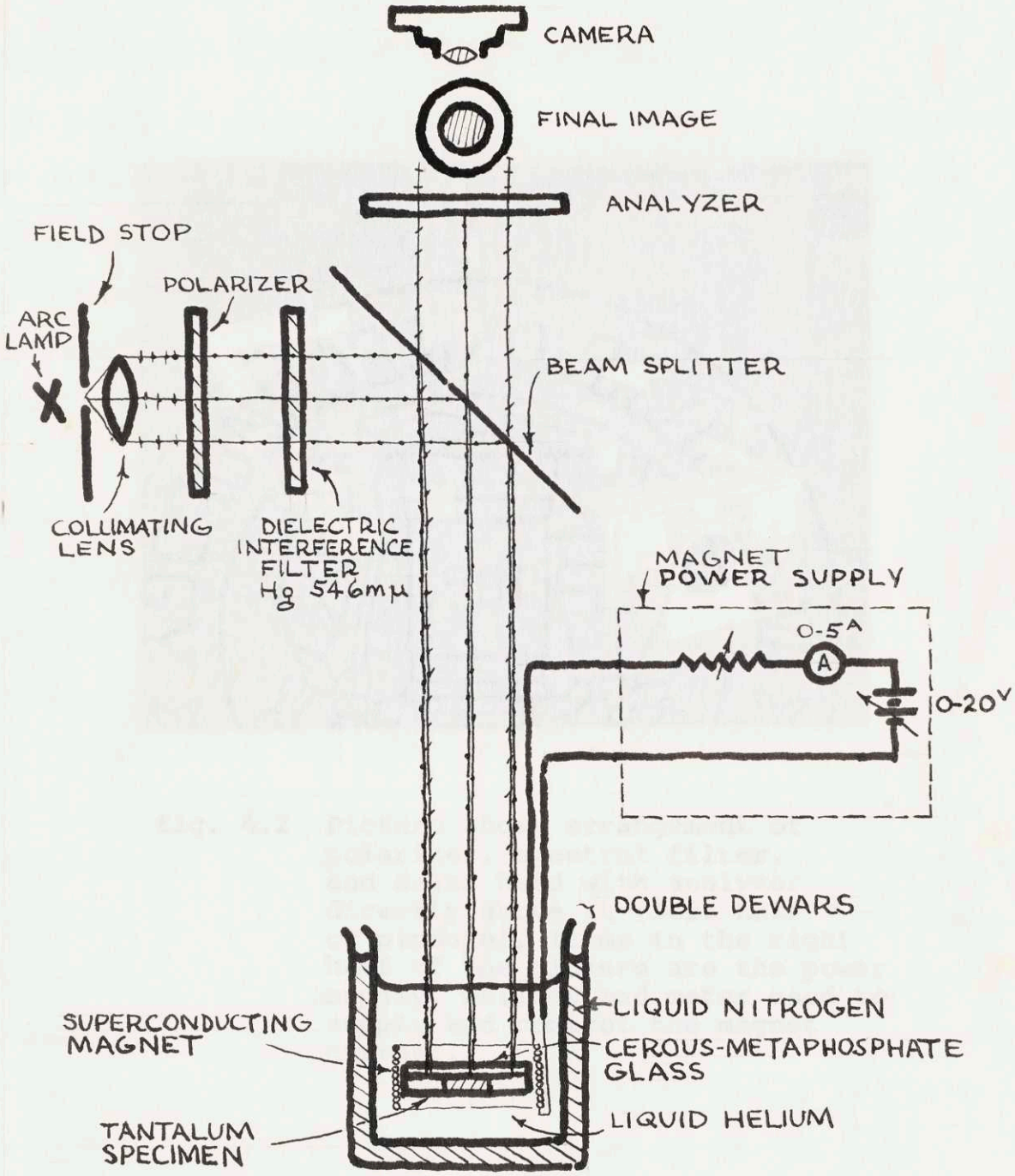

fig. 4.1 Simplified schematic showing arrangement of optical parts.

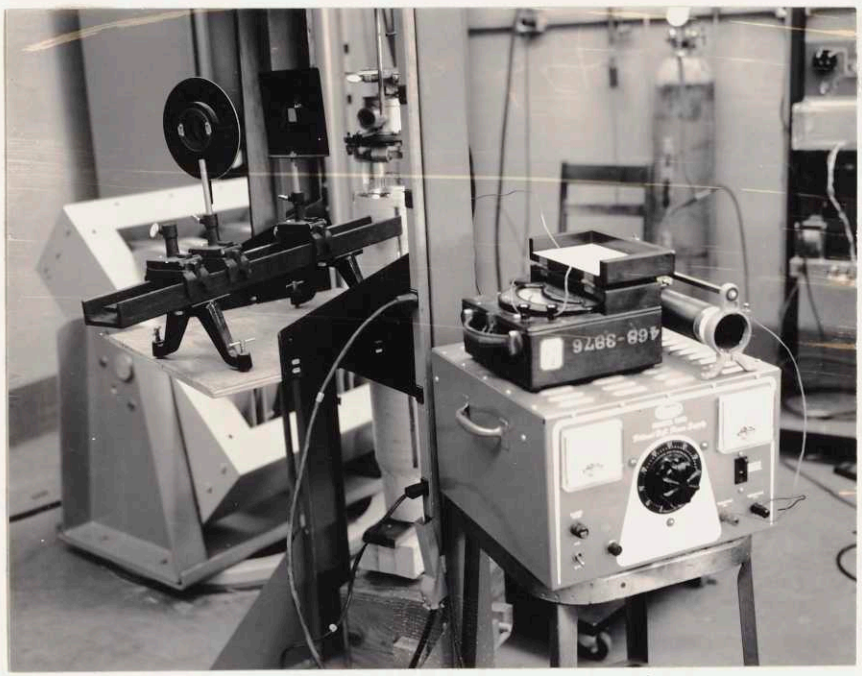

fig. 4.2 Picture shows arrangement of polarizer, spectral filter, and dewar head with analyzer directly above it (left half of picture). Items in the right half of the picture are the power supply, ballast and meter used to supply and control the magnet current.

and developed in UFG for 8 1/2 minutes at 70° F. A photograph of the optical equipment is shown in fig. 4.2.

Mercury Arc Lamp and Associated Power Supply

The source of light used in the experiment is a high pressure Mercury Xenon arc lamp (Hanovia no. 528B). Its maximum rating is 1000 watts and it requires a minimum of about 100 watts to sustain ignition after a 10 minute warmup. Its operating voltage and current is 50 volts and 12 amps (half of maximum dissipation). During the actual experiment the lamp was run at about 80 volts and 12 amps. The lamp power supply is an old magnet supply capable of delivering about 250 volts and 20 amps, thus supplying more than ample power reserve. The arc lamp starter is a commercial item from Hanovia capable of supplying the 20-30 KV necessary to fire the lamp. The lamp housing is a simple metal box with a total volume of about 3 cubic feet. If the lamp dissipation is kept under 900 watts the box provides adequate ventilation for the lamp (no forced air cooling was used with the lamp). A schematic showing the arc lamp power supply circuit is shown in fig. 4.3. The entire lamp assembly is pictured in fig. 4.4. In that photograph the lamp enclosure is on the right, the starter is the small gray box in the lower center of the picture, the magnet power supply is the large black cabinet in the center and the lamp ballast resistor is located in the smaller black box sitting on top of the magnet

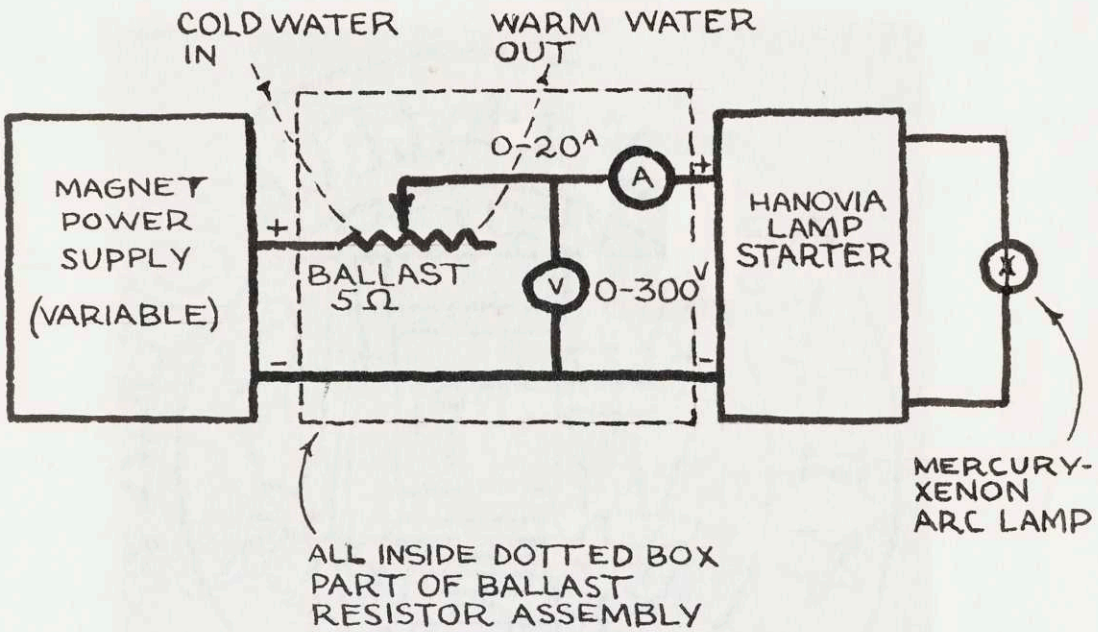

fig. 4.3 Power supply schematic for Hanovia Mercury - Xenon arc lamp.

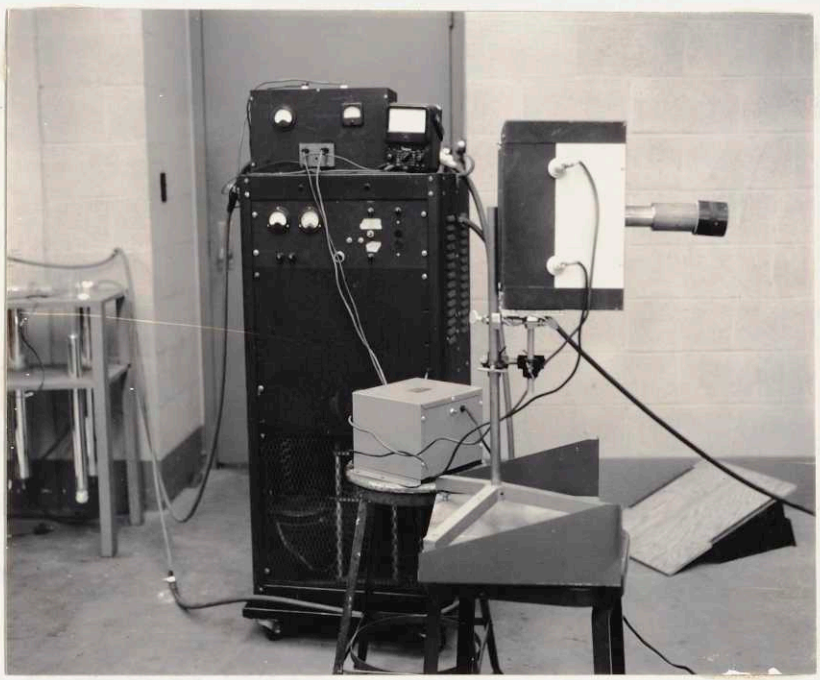

fig. 4.4 Arc lamp and associated power supply, starter, and water cooled ballast resistor.

power supply cabinet. Projecting from the lamp enclosure on the right side are the collimating optics. The optics came from a spot-flood lamp provided by the RLE photo lab.

Dewar Head Assembly

The dewar head is a conventional one which has been modified by the addition of hermetic windows, and a beam splitter mount soft-soldered onto the interior. For pictures of the assembly refer to fig. 4.5. All hermetic seals on the head are made via O-rings except for the viewing window on the top cover (appearing in fig. 4.5a) which was epoxied in place (this was later ascertained to be a mistake as the epoxy cracked under the cold temperatures produced during the Helium transfer). The two plugs appearing on the top cover in fig. 4.5a are hermetically soldered on and provide the power supply connections for the superconducting magnet inside the dewar.

Superconducting Helmholtz Coils

To provide the necessary magnetic fields normal to the surface of the superconductor and to facilitate the placement of the external optics a superconducting magnet designed by John Andrews (presently in Dr. Strandberg's group at RLE) was employed. The magnet is pictured in fig. 4.6. The magnet is wound with Niobium wire in the form of Helmholtz coils - each having 800 turns. The magnet had an experimentally measured field vs current relation of the form

$H = 188\ I$ (H is field in gauss; I = current in amps.)

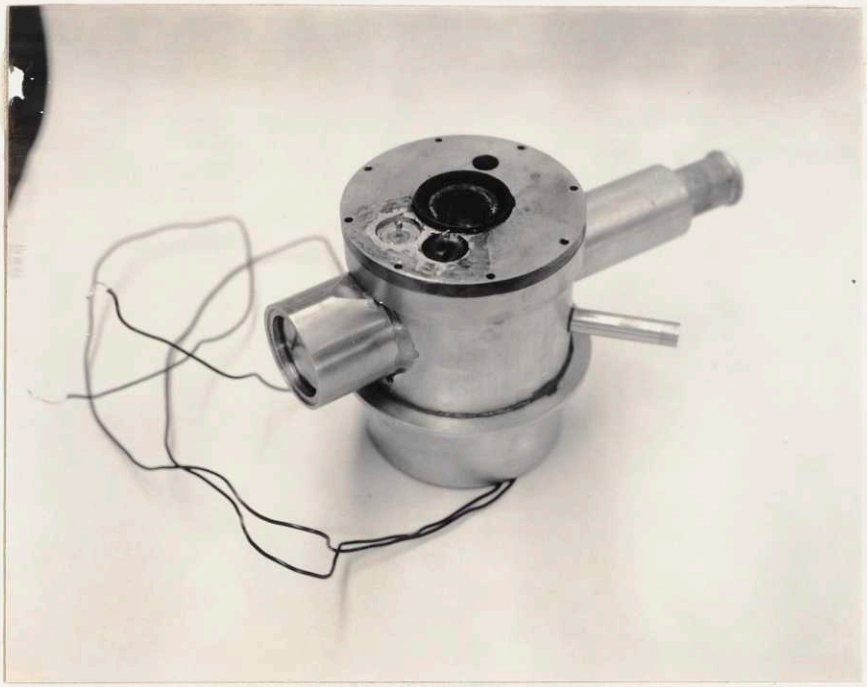

a)

b)

fig. 4.5 Dewar head assembly

a) two hermetic windows are shown (wires are attached to top cover and supply magnet current)- specimen is viewed through top window

b) top cover removed to show beam splitter in its holder

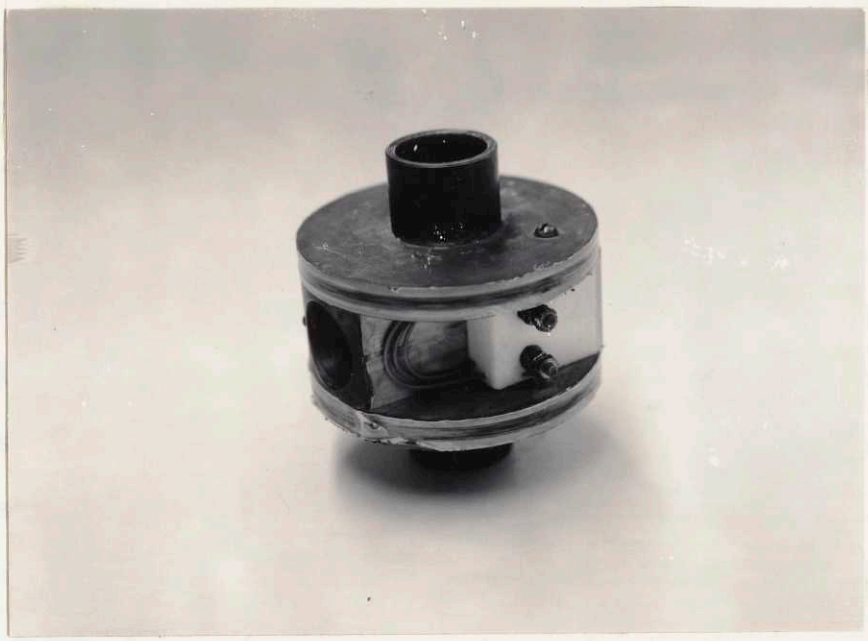

fig. 4.6 Superconducting magnet

Thus, a current of 0.1 amp produces about 20 gauss. Initial tests with the magnet indicate that it can carry about 5 amps maximum before going normal. This corresponds to a maximum field of about 1000 gauss.

Specimen Holder

The specimen holder was simply a long brass tube with a copper plug soldered with wood's metal on the lower end. The top end of the tube was left open. The superconducting specimen sat on a recess in the copper plug at the bottom of the tube. Cooling was thus accomplished by conduction through the copper and radiation loss into the brass tube walls. The liquid Helium was poured around the tube up to about 2 inches from the top - no liquid Helium was introduced into the brass tube. To achieve a leak-proof solder connection between the copper plug and brass tube an ultrasonic soldering iron was employed. The holder is pictured in fig. 4.7.

When pumping on the liquid Helium to get the temperature below 4.2°k a simple Mercury manometer was used to measure the Helium vapor pressure and thus get a measure of the temperature.

The entire experimental assembly (minus camera and tripod) is shown in fig. 4.8.

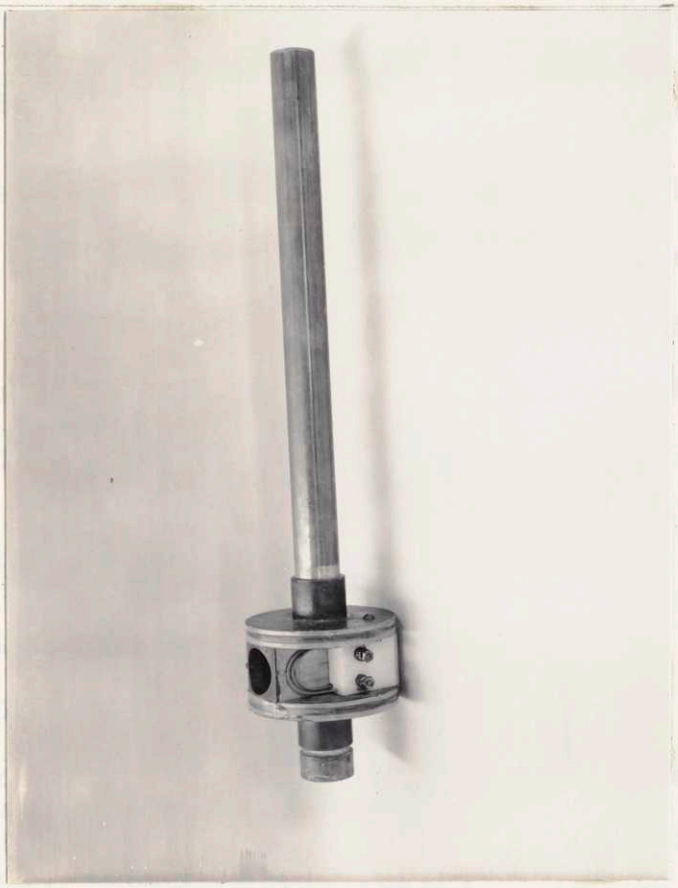

fig. 4.7 Specimen tube inside magnet

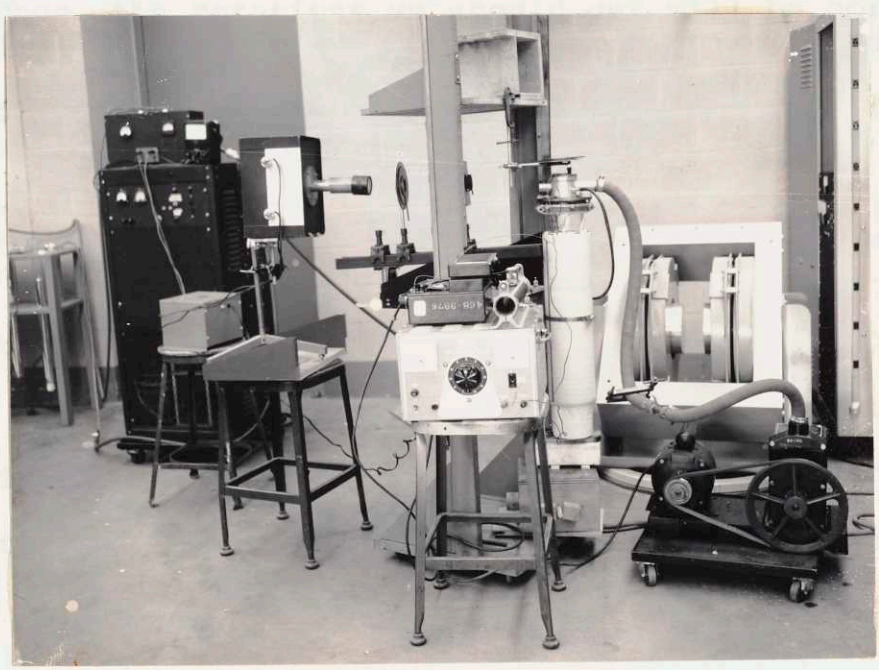

fig. 4.8 Entire experimental setup.

CHAPTER V

EXPERIMENTAL TECHNIQUES AND RESULTS

This chapter will consider the technique employed during the experiment, the materials, and the specimen preparations. The data in the form of domain photographs will be presented. In addition, various tests that were tried with the Cerous Nitrate-glycerol liquid will also be discussed.

The Tantalm Specimen

The metal chosen to investigate for magnetic flux structures was Tantalum. It was chosen because:

1. Cold worked and polycrystalline specimens are known to behave as type II superconductors and hard superconductors though pure single crystals exhibit type I behavior. Thus, we can expect to see an intermediate and mixed state in the same specimen.

2. Tantalum is a high field superconductor (1200 gauss). Thus, the rotations we should get will be correspondingly larger making the domains more easily visible.

3. The metal can be easily machined and polished to form a specimen.

4. The metal has a high transition temperature (4.4°K) thus, eliminating the need for pumping on the liquid Helium to lower the temperature (if need be).

The tantalum was obtained from the RLE machine shop in the form of a cold rolled sheet, 1/8 inch thick, and annealed at 1200°C. The particular specimen was punched out of the sheet and then turned down on a lathe to a diameter of 1/2 inch. So as not to distort the surface structure by mechanically

polishing the specimen the tantalum was used with the original cold rolled finish.

The Paramagnetic Glass

The photographs which are shown at the end of the chapter were all made with a single piece of Cerous Metaphosphate glass 1/2 inch in diameter and 0.5mm thick. The glass was courteously supplied gratis by Dr. Hensler, head of the Ceramics Research Separtment of Bausch and Lomb, Rochester, New York. The glass was quoted to me as having an 80% Cerous Metaphosphate content by weight.

Procedures

The Tantalum specimen was mounted onto the copper block via a small piece of clay. The clay held the specimen in place while at the same time allowing the positioning of the sample so that its surface was normal to the axis of the brass tube holder. A small amount of tape was wrapped about the sample so as to form a holder for the paramagnetic glass. The copper holder was then soft soldered, using wood's metal, onto the brass tube. The tube was then placed in the magnet and the whole assembly lowered into the Helium dewar. The standard flush out and pump out procedure was followed before the Helium transfer. It is especially important that dewars be as clear as possible of any gasses, other than Helium, which might condense out onto the paramagnetic glass surface during the transfer. After the Helium transfer the liquid Helium was immediately

pumped on to lower the temperature to about 2.3°K (corresponding to a Helium vapor pressure of 5cm). As noted in a previous chapter, the lower the temperature the more sensitive the paramagnetic glass. Before the run was started a small electric hot air blower was directed onto the viewing and light admittance windows to defrost them.

About ten minutes prior to the actual run the arc lamp was turned on to allow it to stabilize in intensity. The polarizers were adjusted so that they were slightly off their null or no transmittance position. Going from a position on one side of the null to the other had the effect of producing the negative image of what appeared on the other side of the null. The choice of which position to chose was merely one of deciding what image was more easily photographable.

A comment on Certain Mistakes Made

Prior to the first successful runs with the Tantalum there had been a certain number of runs which proved to be dismal flops. It should be emphasized that Tantalum (non single crystal, cold worked) can very easily exhibit the properties of a hard superconductor. That is, once magnetized, it remains magnetized, even though the external field is removed. The trapped in flux can only be removed by either raising the temperature of the specimen above its critical temperature or reversing the magnetic field applied to the material. Thus, the original runs were failures as the Tantalum was inadvertently magnetized when the

superconducting magnet was innocently tested before each run. As the field was not reversed during these runs the Tantalum showed no visible domain structure to our dismay.

Another series of time consuming mistakes which were made concerned original tests using the Cerous Nitrate Glycerol liquid. As indicated by Alers the liquid, to be useful, should have about 75% of the Cerium compound by weight present in the mixture. Original samples of the Cerous Nitrate obtained from City Chemical in New York proved to be highly impure. Rather than being able to dissolve 3 grams of the chemical in 1 gram of the glycerol, somewhat less than 1/3 gram of the chemical was capable of being dissolved in the same amount of glycerol. This solubility problem was solved with the purchase of the chemical from a new company. As is always the case, the elimination of one problem introduces ten more. The new chemical, though it was highly soluble in the glycerol, introduced a great deal of ultra-small air bubbles into the solution. As the liquid with the Nitrate in it was quite viscous the bubbles refused to separate from the solution. Pumping on the liquid removed the larger bubbles but merely homogenized the smaller ones in the solution. Heating the solution did appear to remove the bubbles and make the liquid somewhat clearer, but a certain amount of decomposition of the nitrate was evident in the yellowish color which appeared, (the heating was done in boiling water). Another problem arose when the solution was poured over the sample, (a small retaining ring was used to

contain the liquid), and everything put into the dewar ready for the usual flush, pump-out procedure before the Helium transfer. Pure glycerol does not appear to boil when the pressure over it is reduced to several millimeters of Mercury. However, a glycerol solution containing 75% nitrate in solution does boil when the pressure above it is reduced to several centimeters of Mercury. This boiling phenomena only succeeds in spilling the solution all over the inside of the specimen holder. Even when a small amount of the solution did remain on the sample, it did not freeze into a transparent glass but fractured into hundreds of small glassy pieces from the thermal stresses, thus making observation of the Tantalum impossible. The liquid scheme was subsequently dropped in favor of the glass.

Photographic Sequence of Domain Structures

Using the paramagnetic glass obtained from Bausch and Lomb the following set of sequence photographs were obtained during one run. It should be noted that although six pictures appear on each page except the last one, there are only three independent photographs on each page. Each picture appears twice. One photograph has been printed sharp while the other has been printed slightly out of focus. Interestingly enough, the out-of-focus picture appears in certain instances to reveal more of the domain structures than the sharp print. Apparently printing the pictures slightly out of focus has the effect of adding a low-pass optical filter. The high spatial frequency photographic grain patterns disappear while the relatively low

frequency domain patterns remain if not emphasized a bit.

All the pictures are straight prints from the negatives. Streaks that appear in some of the photographs were stray reflections off the many optical windows and mirrors that were between the camera and the specimen. The actual image size on the negatives was somewhat less than 1/8 inch. All the pictures are straight prints from the negatives. Printing exposures for all the pictures are, however, not the same. In the actual run, the exposure for each negative shot was 1 sec at f3.5.

During the experimental run the magnetic field was slowly increased from zero up to about 800 gauss and then slowly decreased to zero. The current leads to the magnet were reversed and the field increased one again to about 800 gauss but in the opposite direction. The field was then abruptly reduced to zero.

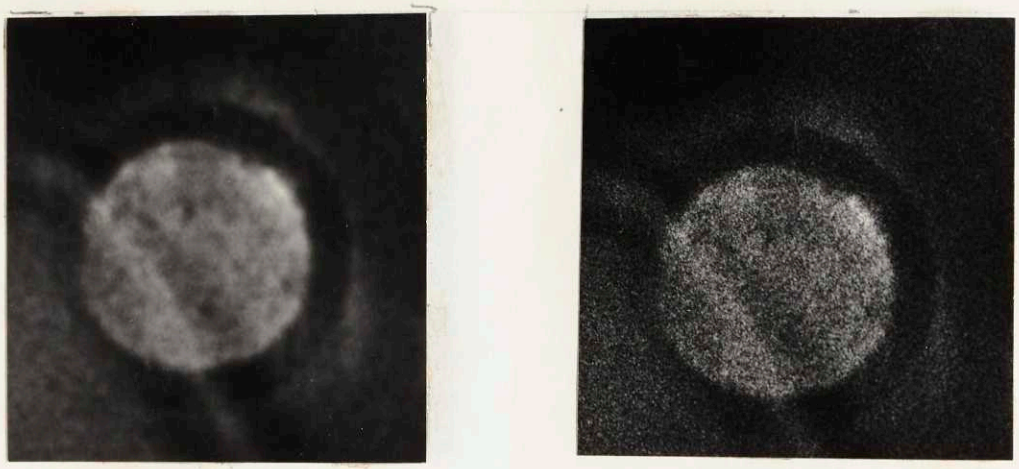

fig. 5.1 Tantalum - field increasing - 507 gauss

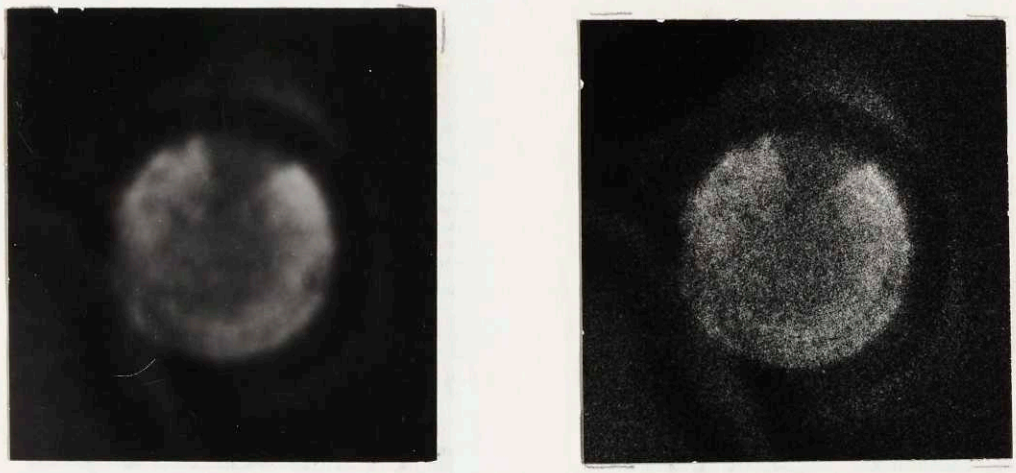

fig. 5.2 Tantalum - field increasing - 658 gauss

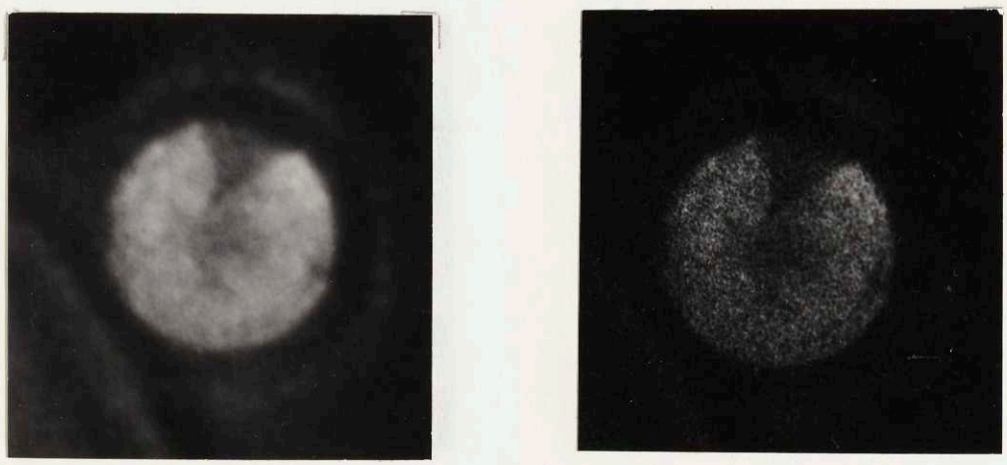

fig. 5.3 Tantalum - field increasing - 752 gauss

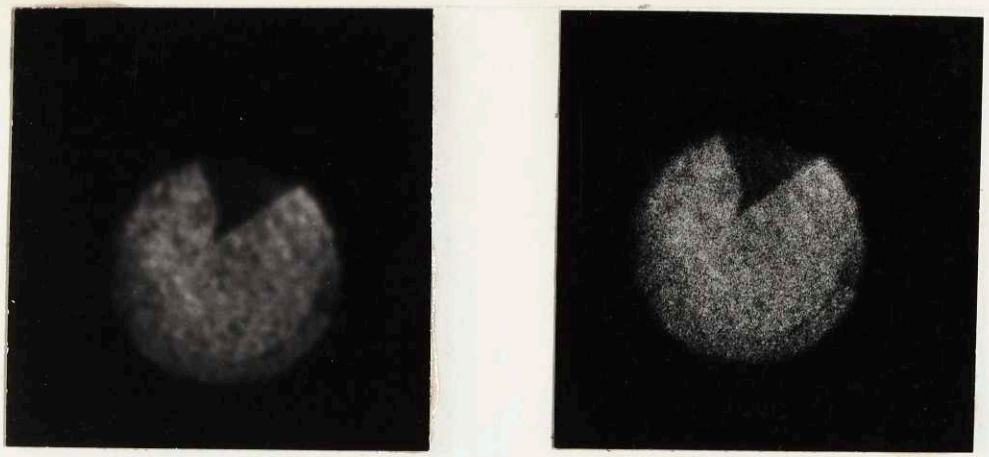

fig. 5.4 Tantalum - field increasing - 846 gauss

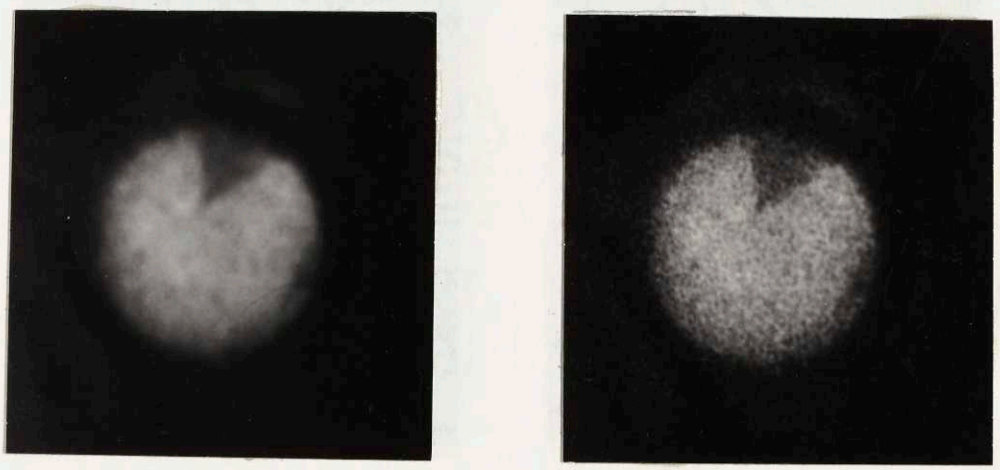

fig. 5.5 Tantalum - field decreasing - 376 gauss

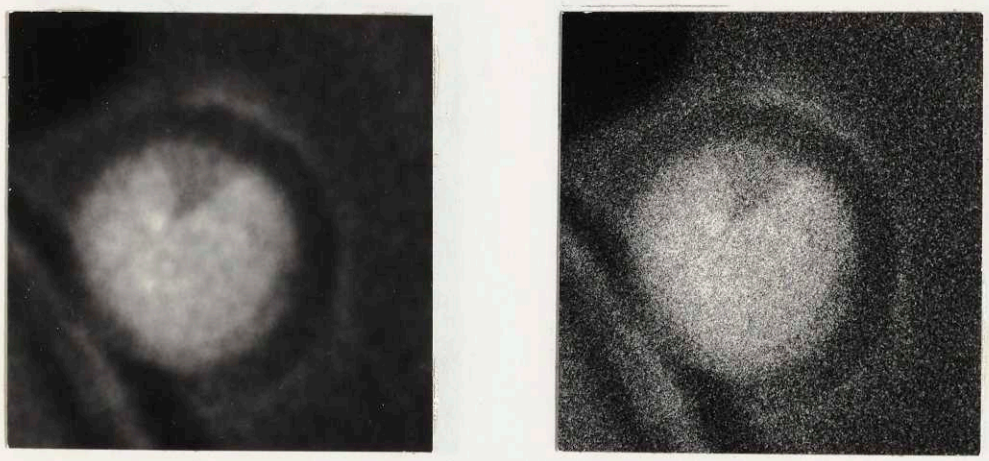

fig. 5.6 Tantalum - field decreasing - 0 gauss

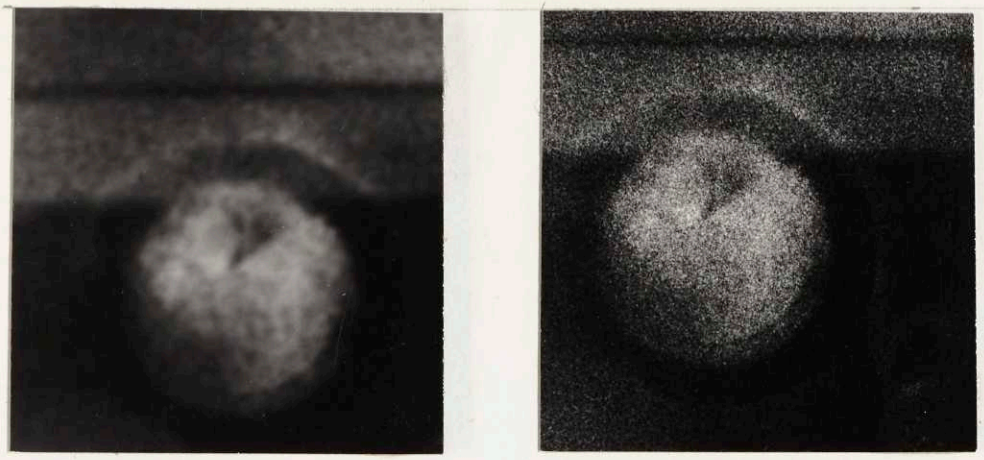

fig. 5.7 Tantalum - reverse field increasing - (-38 gauss)

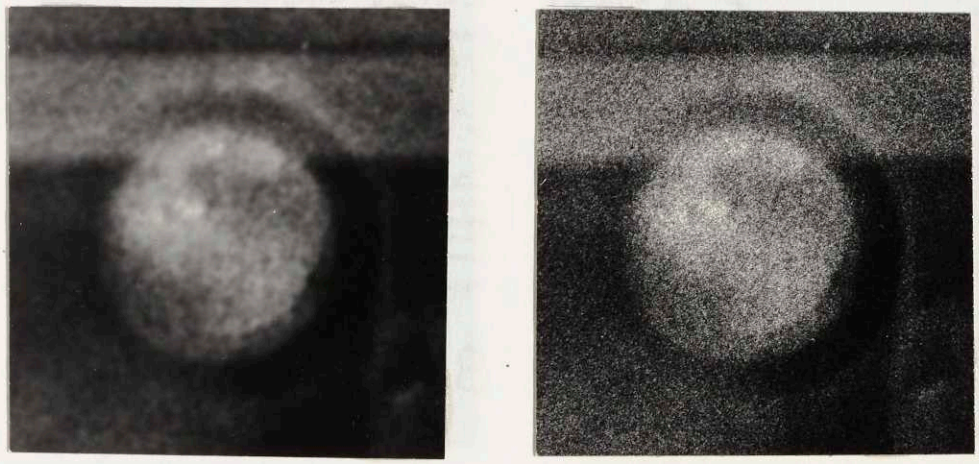

fig. 5.8 Tantalum - reverse field increasing - (-132 gauss)

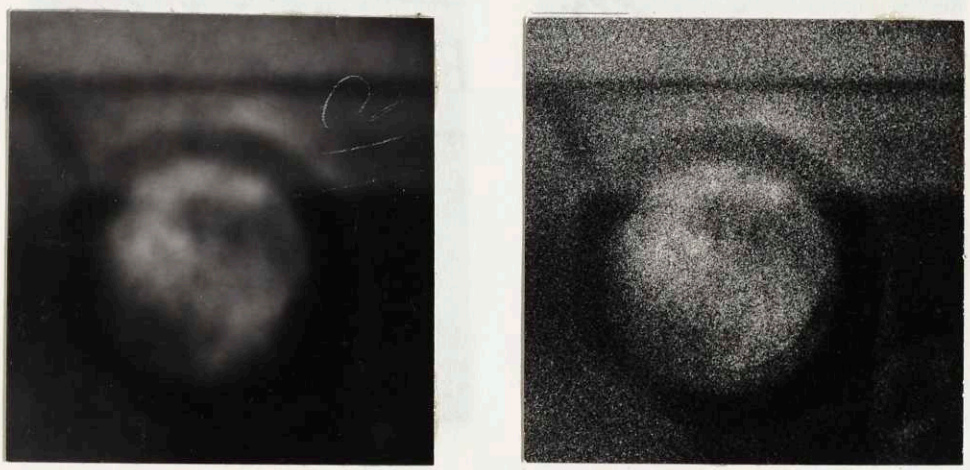

fig. 5.9 Tantalum - reverse field increasing - (-188 gauss)

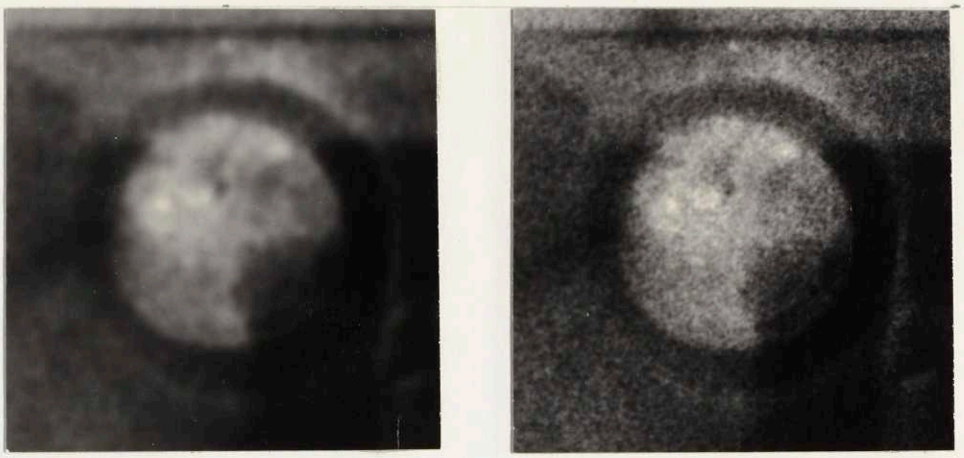

fig. 5.10 Tantalum - reverse field increasing - (-282 gauss)

fig. 5.11 Tantalum - reverse field increasing - (-320 gauss)

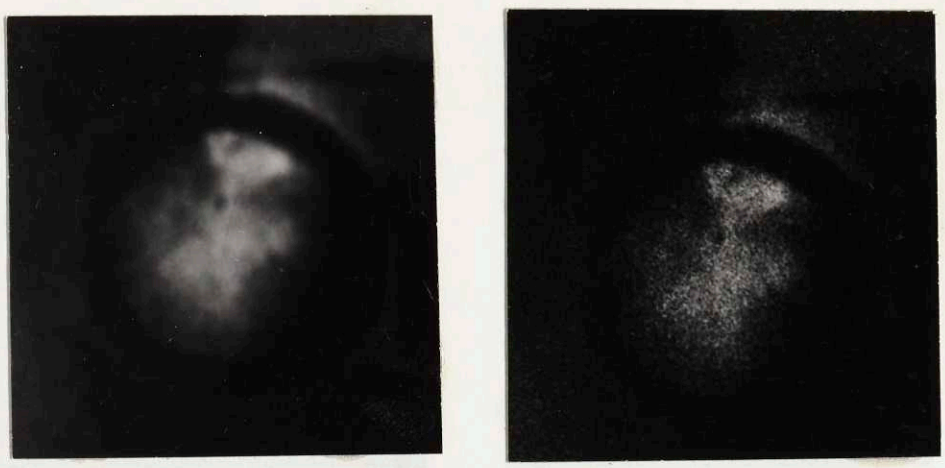

fig. 5.12 Tantalum - reverse field increasing - (-564 gauss)

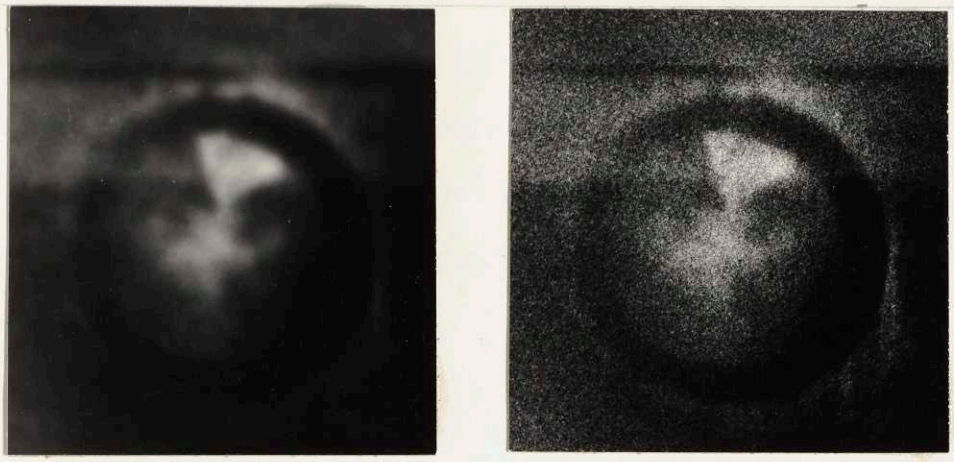

fig. 5.13 Tantalum - reverse field increasing - (-752 gauss)

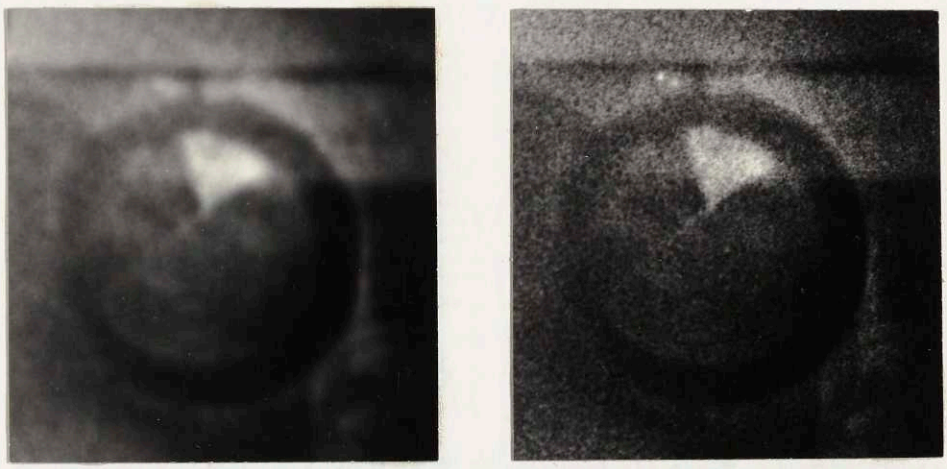

fig. 5.14 Tantalum - reverse field increasing - (-827 gauss)

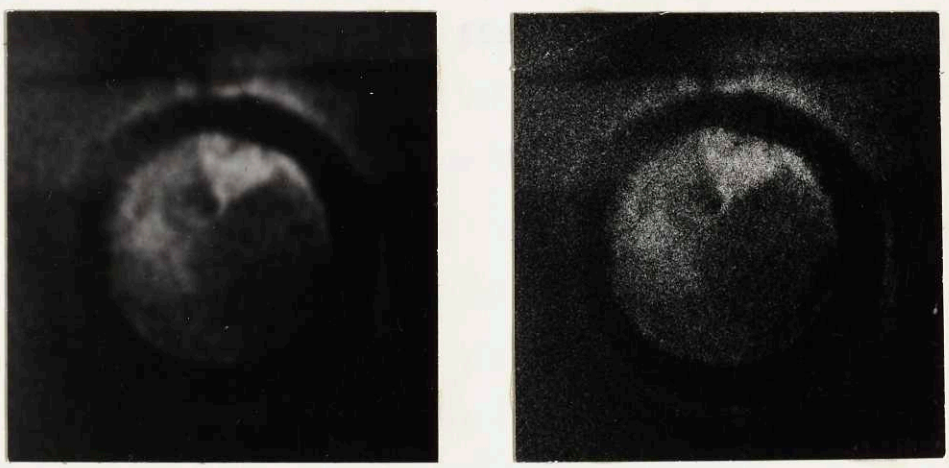

fig. 5.15 Tantalum - field reduced from -827 to 0 gauss suddenly

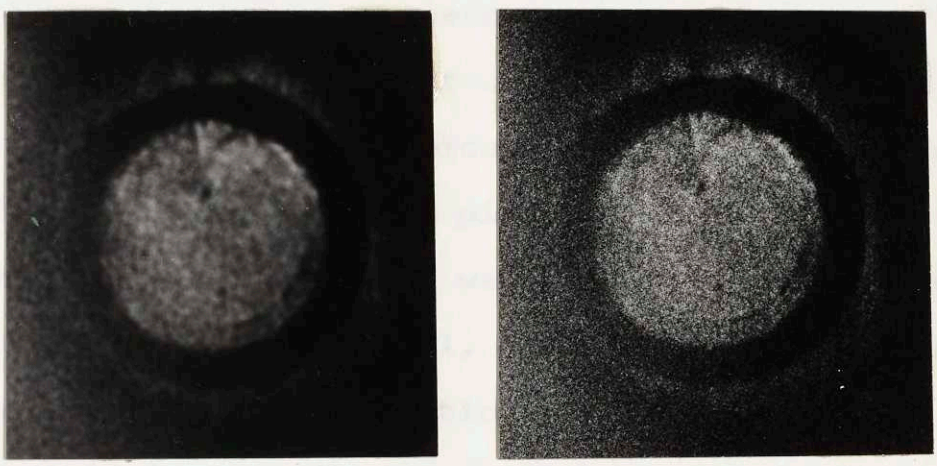

fig. 5.16 Tantalum - zero field - temperature raised to 4.2°K

CHAPTER VI

DISCUSSION OF RESULTS

This chapter will present an analysis of the set of photographs which appeared at the end of the last chapter in light of what we know about the various magnetic states of the superconducting metal.

Appearance of the Intermediate State

It appeared visually while the pictures were taken that the intermediate state seemed to appear at a field strength of about 507 gauss. The photographs show, however, that the intermediate structure had already progressed across about a tenth of the diameter of the specimen. It seems apparent that the actual start of the structure was closer to 350 gauss than 500 gauss. What was apparent while the pictures were taken but does not show up in the photographs was that the appearance of the intermediate state was a gradual, continuous phenomena as compared with the reverse magnetization phenomena which took place in very rapid jumps. The intermediate state structure as shown in the first three of the photographs shows the structure extending in a series of irregular finger-like projections (they seem to show up a little better in the pictures which are slightly out of focus). The patterns seemed to follow the field changes in that when the field was kept constant the patterns did not appear to change or move.

****

Please note that in all the pictures there seems to be a pie shaped region appearing near the top of the picture - this is

not part of the domain structure, but, merely a region where a small piece of the paramagnetic glass was removed. This now allows us to monitor the rest of the glass with regards to flux trapping. When the pie shaped region can no longer be seen it means that the glass is no longer magnetized in that area and hence, the metal is either superconducting there or contains a very small amount of trapped flux.

****

Appearance of Gray Regions

What appears apparent in the first four pictures is that there are numerous white "spots" or areas in a gray region and that both appear to make up the intermediate state. These areas are to be contrasted with the somewhat darker interior of the tantalum disk which is still superconducting (at least in pictures 1-3). As photographs 5 and 6 show considerable flux trapping even down to zero field it is apparent that the metal is behaving as a typical hard superconductor. In apparent agreement with DeSorbo's results these gray regions are most likely parts of the mixed state. Picture number 2 seems to show this gray region surrounding the inner dark superconducting core while in picture number 3 the gray regions seem to cover the entire specimen.

Reverse Magnetization

Pictures 7-14 are quite interesting in that the boundary motion which took place occurred in abrupt jumps. These sequence of pictures represent the specimen during the reverse magnetization procedure. It was easily noted during the run that entire

sections of the specimen would become normal almost instantaneously in contrast to the initial magnetization. Pictures 8-10 are interesting in that the pie shaped monitor section is no longer visible indicating that the glass was not magnetized in that particular region. The reverse field strength at which the monitor region appeared to disappear was -132 gauss. This flux value is to be compared with the initial 350 gauss at which it is estimated the flux first started to penetrate the Tantalum disk. The hysterisis of the sample is quite evident. It, thus, represents a breakdown of the Meissner effect. This flux-trapping or "incomplete" flux exclusion is also apparent in the "soft" type-I superconductors such as lead and tin but is not as great there. The reverse field strength at which the specimen once again seemed to be completely magnetized was -827 gauss. This value is comparable to the initial magnetization on the virgin run.

Apparent Demagnetization by Quick Flux Changes

Pictures 4-6 show the resulting trapped flux that remained when the field was slowly reduced to zero on the virgin run. At zero field the specimen seems to have lost some flux, but, nevertheless, the specimen is still "uniformly" magnetized. These pictures are to be compared with picture 15 in which the reverse flux was abruptly reduced from -827 gauss to zero gauss. The picture shows an apparent demagnetization on the left side of the specimen. Most likely the abrupt change in field induced eddy currents of sufficient strength in the copper sample holder so that there was enough of a temperature rise in the

sample to provide paths for the flux to escape. The temperature effect seems a logical explanation in light of picture 16 which shows the decrease in flux as the sample temperature is brought up to $4.2^{\circ}K$.

Demagnetization Coefficient

As indicated in a previous chapter the ratio of applied field to the critical field is related to the demagnetization coefficient by the equation

$$\frac{H_{app}}{H_c} = 1 - D$$

As field penetration was estimated to start at 350 gauss and end at about 850 gauss the value of the demagnetization coefficient is then $D = 0.59$.

Suggestions for Further Research

The use of a single specimen of Tantalum is an obvious handicap in investigating the magnetic domain patterns. Further tests need to be done on specimens which have undergone various mechanical preparations. It should be pointed out that the pictures were all taken without depositing a mirror film on the paramagnetic glass. This is in contrast with DeSorbo's pictures which were all made with the glass aluminized on one side. Thus, it is apparent that the technique works without need for a mirror surface to reflect the light back. This can be a decided advantage in studying the effects of crystal size, grain boundaries, and cold working on the intermediate and mixed states. We can now electropolish a specific specimen, etch it to bring out the grain boundaries

and then place the paramagnetic glass directly onto this etched surface. The grain patterns (possibly distorted by cold working) can now be correlated with the observed magnetic domain patterns. This has not been done in any of the literature and would make a very easy extension of the work that has already been done.

At the very best the pictures in the previous chapter show a spatial resolution of about 0.5mm. DeSorbo's pictures are somewhat better in that they show a resolution of 0.2mm. It would make an interesting research project to consider the design of an experiment which would perhaps increase the resolution down to perhaps 10 microns. With such resolution it might be possible to resolve any detail in both the intermediate and mixed states. As pointed out previously, greater resolution of say 10 microns requires that the paramagnetic layer on the superconductor be no thicker than 10 microns. This would now seem to say that the specific rotation would be about 100 times less than it is now. It is suggested that the specific rotation can be increased with such a thin paramagnetic layer by forming a resonant Fabry Perot optical filter on the surface, the paramagnetic material can form the dielectric spacer, and another metallic or dielectric film can form the other mirror surface. With such a structure it should be possible to magnify the specific rotation.

REFERENCES

1. DeSorbo, Cryogenics, 4,257 (Oct. 1964)

2. A. G. Meshovsky, A. I. Shalnikov, J. Exptl. Theoret. Phys. (USSR) 17, 851 (1947)

3. A. G. Meshovsky, A. I. Shalnikov, J. Phys. (USSR) #, 1 (1947)

4. A. L. Schawlow, G. E. Deulin, Phys. Rev., 110, 1011 (June 1, 1958)

5. P. B. Allers, Phys. Rev., 116 1483, (Dec. 1959)

6. P. B. Allers, Phys. Rev., 105, 194 (Jan. 1957)

7. Y. B. Kim, Physics Today, (Sept. 1964)

8. Alers, Phys. Rev., 105, 104 (Jan. 1957